

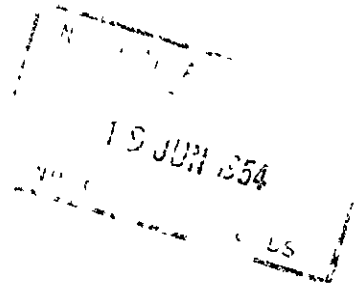
National

LIBRARY

CP No 29

(12,883)

ARC Technical Report



MINISTRY OF SUPPLY

AERONAUTICAL RESEARCH COUNCIL

CURRENT PAPERS

THE LOW SPEED PERFORMANCE OF RELATED AEROFOLS IN CASCADES

By

A D S. Carter

Crown Copyright Reserved

LONDON · HIS MAJESTY'S STATIONERY OFFICE

1950

Price 3s. 6d net.



Report No. R.55.

September, 1949.

NATIONAL GAS TURBINE ESTABLISHMENT

The Low Speed Performance of Related Aerofoils in Cascade

- by -

A. D. S. Carter

SUMMARY

This report contains a general analysis of some test results on compressor and turbine cascades. It is shown that both these types of cascades can be treated in a similar manner, and data is given from which the performance of any cascade of the related series of aerofoils considered can easily be calculated. An attempt has been made to explain variations in behaviour of cascades, and, appreciating the factors involved, a fair idea of the performance of other aerofoil sections can be obtained.

RESTRICTED

LIST OF CONTENTS

	<u>Page.</u>
1.0 Introduction	4
2.0 Estimation of Optimum Incidence and Deflection	6
2.1 Optimum Incidence	6
2.2 Deviation and Deflection	7
3.0 The performance at Optimum Incidence	8
3.1 Pitch/chord - Thickness Correction.	8
3.2 The Stagger Correction	8
3.3 Scale Effect	9
3.4 Performance Curves	10
4.0 The Performance at Other Incidences	10
5.0 Effect of Some Modifications in Profile Shape	11
5.1 Maximum Thickness	12
5.2 Maximum Camber	12
6.0 Some General Comments	13
7.0 Conclusions	14
References	15

LIST OF APPENDICES

<u>Appendix</u>		<u>Page.</u>
I	Notation	17
II	The Calculation of Cascade Characteristics	19

LIST OF ILLUSTRATIONS

<u>Fig</u>	<u>Title</u>
1	(a) Base Aerofoil Cl (b) Vortex Representation of Cascade
2	Normal velocity coefficient
3	Value of $10PT_{\infty}$ for various Cambers
4	Value of $10PT_{\infty}$ for various Cambers
5	Optimum Incidence at Infinite Pitching
6	Deviation Rule
7	Effect of Stagger on Cascade Performance
8	Examples of Stagger Effect
9	Lift Drag Ratios ($\alpha_2 = -60^\circ$ and $\alpha_2 = -40^\circ$)
10	Lift Drag Ratios ($\alpha_2 = -20^\circ$ and $\alpha_2 = 0^\circ$)
11	Lift Drag Ratios ($\alpha_2 = +20^\circ$ and $\alpha_2 = +30^\circ$)
12	General Performance Curves
13	Performance Curves (s/c = 0.5)
14	Performance Curves (s/c = 1.0)
15	Performance Curves (s/c = 1.5)
16	Incidence Increment ($\alpha_2 = -60^\circ$ and $\alpha_2 = -40^\circ$)
17	Incidence Increment ($\alpha_2 = -20^\circ$ and $\alpha_2 = 0^\circ$)
18	Incidence Increment ($\alpha_2 = +20^\circ$ and $\alpha_2 = +30^\circ$)
19	General Incidence Increment Curves
20	Loss and Deflection v Incidence
21	(a) Effect of Aerofoil Thickness on Cascade Performance (b) Optimum Position of Maximum Camber
22	Combinations of Fluid Outlet Angle and Position of Maximum Camber
23	Cascade Performance
24	Comparison of Test and Calculated Characteristics
25	Comparison of Test and Calculated Characteristics
26	Comparison of Test and Calculated Characteristics

1.0 Introduction

Although the modern approach to axial compressor and turbine design has resulted in the fairly extensive testing of cascades of aerofoils, there is, as yet, no comprehensive theory connecting all the test results on the widely differing types of cascades encountered in general practise. Several rules have been proposed^{1,2,3} which ensure a satisfactory design of cascade to fulfil given functions, and these have been of considerable practical importance. Their greatest disadvantage, however, has been their inability to express quantitatively the result of small changes from the recommended values. They have also tended to over simplify the problem to a certain extent. On the other hand they have shown that most types of cascades can be put on to a common footing, while at the same time avoiding complex and lengthy calculations. This report extends such work and attempts to build up a rational explanation of the behaviour of all types of cascades, and presents methods that will enable the performance of any cascade having practical importance to be readily estimated.

It is important, however, that the limitations which have been arbitrarily imposed on the analysis should be noted from the outset. It seemed quite clear to the author that if exact results were desired some of the more refined methods used in conventional aerodynamics would have to be employed. Methods of conformal transformation or extensions to the thin aerofoil theory, together with the solutions of the boundary layer equations, immediately suggest themselves in this connection. It is well known, however, that these methods involve lengthy calculations, often extending over several weeks before any useful results can be obtained. For a designer of multi-stage axial compressors and turbines who may have to consider the performance of several hundred cascades before the design is finalised, such a procedure is clearly out of the question, and there is a great need for a simplified theory which can give results, even if only to the first degree of approximation, over a very wide range with a minimum of computation.

It can be argued that simple interpolation of existing test results could be used. This is undoubtedly a very powerful method, but unfortunately, due to the large number of variables involved it can only be used in very limited circumstances, and considerable difficulty is often experienced in practice owing to the lack of a systematised series of tests between which to interpolate.

Consistent with the overriding conditions there are a number of ways of approaching the general problem. The first and most obvious method is based on the assumption that the cascade consists of a series of curved channels. By consideration of the performance of diffusing or accelerating bends the performance of the cascade can then be found. Apart from the difficulties connected with the correct definition of the passage, this method does not seem to yield any very satisfactory results consistently. It would appear that each channel cannot be considered as an isolated entity but only in relation to its position in the cascade as a whole. With this condition to be satisfied the analysis enters a rather detailed and lengthy stage, and it is not considered worth following from a practical point of view.

The second basic method of approach consists of relating the performance of the complete cascade to the performance of the individual aerofoils at infinite pitch, i.e. the isolated aerofoil. For very wide pitching it is found sufficient to assume the same characteristics for the cascade as for the isolated aerofoil, using the incidence based on the vector mean velocity for the cascade as corresponding to the incidence of the isolated aerofoil measured in the normal way. For closer pitching however the method breaks down. Attempts have been made to overcome this difficulty by the introduction of a number of empirical factors, but no satisfactory results could be obtained without losing all relation to the physical conditions.

A more refined method of approaching the problem is to replace each of the aerofoils, apart from the central one, by vortices concentrated at the centre

of pressure of the aerofoils. The performance in this modified field of flow can then be estimated more accurately than is possible with simple vector mean velocity calculations. This method was developed by Betz⁴, who derived several charts to facilitate the computation. Here again, however, the method failed to cover a sufficiently large range with a suitable degree of accuracy. Obviously a greater degree of approximation can be obtained by using more vortices with which to replace the aerofoil, and so developed a series of methods by Pistolesi⁵, Ackeret⁶, Katzoff Finn and Lawrence⁷, Dicsendruck⁸ etc., of varying degrees of accuracy, but all needing excessive computation before satisfactory results can be obtained. Nevertheless it was felt that this approach had a fairly sound theoretical background, and a further investigation along these lines was conducted.

The method of analysis finally evolved and presented in this report is based fundamentally on the vortex replacement idea. One of the exact mathematical expressions derived by Betz has, however been replaced by an empirical one derived by successive approximations from the test results. Furthermore, the exact mathematical significance of the solution has not been rigorously adopted: for instance, although the method purports to relate the cascade aerofoil with the isolated aerofoil, the isolated aerofoil in this case is an hypothetical one, and can have no real existence from which measured results can be taken. It does, however, form a common denominator which will enable us to move freely from one cascade to another. The lack of real existence prohibits the direct use of isolated aerofoil characteristics, and the performance of the hypothetical aerofoil can only be deduced indirectly from the cascade results. This is rather important, in as much as the ideal case is still far from being achieved, when aerofoils need only be tested at infinite pitch and the cascade characteristics deduced therefrom.

The main analysis presented in this report has been carried out on the related series of aerofoils obtained by superimposing the C.1 base profile on circular arc camber lines. The co-ordinates of this profile are given in Fig.1(a), and the method of constructing the aerofoil in Appendix I. The results would apply equally well, however, if the C.2 or C.4 base profiles were used.

For the most part the general analysis was carried out on results published in references 3, 9, 10, 11, 12 and 13, though the results contained in references 14, 15, 16 and 17 together with some unpublished results were also referred to. In any general analysis of cascade tests one immediately runs into difficulties arising from unknown tunnel interference effects, due either to different secondary flows or different degrees of turbulence, and also into difficulties arising from the different manufacturing standards applied to the blades themselves. The first series of results quoted above were considered to be the most consistent, and consequently the analysis was concentrated on these. Generally speaking they are what may be called "good" results, and it is unlikely that a better performance could be obtained without exceptional care in manufacture of the blades etc. In applying this analysis to practical problems allowance should be made for these conditions. The results used in the analysis all refer to an effective Reynold's number of about 4×10^5 , based on outlet velocity and chord.

Although the analysis of test results from these related aerofoils forms the main theme of the report, some results and comments are presented in the concluding paragraphs on the effect of changes in the profile contour.

Except for one modification standard notation has been used through this report. It has been repeated in Appendix I for reference. The exception is the use of the term "loading factor", denoted by ψ , in place of the more lengthy expression "lift coefficient based on outlet velocity", denoted, in ref.3, by $C_L(V_2)$.

2.0 Estimation of Optimum Incidence and Deflection

2.1 Optimum Incidence

Before dealing with the actual analysis it is necessary to define exactly what we mean by optimum incidence. Generally speaking, in their practical application, cascades are operated at the highest possible deflection compatible with a reasonably low value of the energy loss through the cascade, i.e. without stalling. Stalling of a cascade is assumed to occur when the blade loss is twice its minimum value. This is a purely arbitrary figure but allows an exact means of definition. Obviously it is inadvisable to operate right on the stalling point, and so a nominal deflection (ϵ^*), defined as 0.8 of the stalling deflection (ϵ_s) is often used for design purposes (see reference 18 for instance). While eminently satisfactory from a compressor or turbine design outlook; this definition is again without much fundamental significance. We shall therefore define "optimum incidence" as that incidence at which the maximum value of the lift/drag ratio occurs. This avoids all reference to stalling and has some fundamental significance, representing the point at which the opposing pressure gradients on the upper surface of the aerofoil are becoming too large for efficient operation

Now it is well known that for infinitely thin aerofoils the incidence for maximum lift/drag ratio is that at which the front stagnation point is situated at the leading edge, since under these circumstances steep opposing pressure gradients are avoided. While there is no definite corresponding criterion for thicker aerofoils with well rounded leading edges, it would appear that the flow round the leading edge is criterion of the relative quality of the overall flow conditions. Furthermore the flow conditions round the leading edge are determined once the position of the stagnation point is known. It can be concluded, therefore, that as with thin aerofoils so with thick aerofoils, the position of the front stagnation point is a criterion for optimum incidence, though in this latter case the stagnation point will probably not be exactly at the leading edge. (Examination of a number of cases has shown it is near the leading edge, just on the lower surface).

Suppose, then, we have a cascade operating at the incidence giving maximum lift/drag conditions, and we wish to change, say, the pitching of the cascade. If, as the pitch was changed, we could also change the direction of the incident air stream such that the front stagnation point remained fixed on the aerofoil contour, we should in all probability find that the new incidence would be the correct one for maximum lift/drag conditions at the new pitching. We have at our disposal, therefore, a method of making small changes to cascade geometry, and still being able to determine the optimum incidence; and what is more, the method is dependent only on the potential flow round the aerofoil. While this can be determined theoretically, the standard methods of solving the problem are, as stated in Section 1.0, too lengthy for practical application, and so the following modification to the vortex replacement method was devised to facilitate calculation.

Consider a cascade of aerofoils operating at optimum incidence, concentrating in particular on any one aerofoil of the series, which we will place at the origin. We can replace each of the other aerofoils by vortices of equal circulation, situated at the centre of pressure of the actual aerofoils, as shown in Fig.1(b). The central aerofoil will be acting in the flow field of these vortices, the potential function of the field being given by⁷

$$\omega = \frac{iK}{2\pi} \log \left\{ \text{Sin} \left(\frac{\pi z}{a} \right) / z \right\} \dots\dots\dots(1)$$

The change in air direction at any point brought about by this field is given approximately by⁴

$$\Delta \alpha = v_n / V_m \dots\dots\dots(2)$$

where v_n is the velocity perpendicular to the radius vector at that point. In particular, for the leading edge

$$\Delta i = v_n / V_m = \frac{v_n^* \times C_L}{2 s/c} \text{ rad} \dots\dots\dots(3)$$

Values of v_n^* (equal to value of v_n for unit circulation and pitching) as derived from equation (1) have been charted by Betz⁴.

Now suppose that the pitching of the blades is changed slightly; Δi will be changed accordingly, and in order to keep the stagnation point fixed as this change is being made, we must give an equal and opposite change to the incident air stream i.e.

$$i_{opt} - i_{opt}' = \Delta i - \Delta i' \dots\dots\dots(4)$$

where the dashed symbols refer to the new conditions. Δi and $\Delta i'$ can be calculated from equation (3) above. Alternatively, referring to infinite pitch, $\Delta i' = 0$ and so

$$i_{opt} = i_{opt\infty} + \Delta i \dots\dots\dots(5)$$

Since stagger can have no effect on the flow at infinite pitch, the optimum value of $i_{opt\infty}$ is a constant for any given blade. Hence the optimum incidence can in theory, be calculated for any cascade so long as $i_{opt\infty}$ is known for the particular blade.

Using the theoretical values of Δi , $i_{opt\infty}$ was calculated for each type of aerofoil of the test results quoted in section 1.0. The aerofoils for which the test results covered a wide range of pitching and stagger showed a considerable scatter in the values of $i_{opt\infty}$. It was noticed, however, that it was always stagger which produced the most marked variation, and that similar tendencies were apparent for all types of aerofoils. A mean value was therefore assumed for each aerofoil, and a few function of v_n^* calculated. A mean value of this function was assumed, and by repeating the process several times an empirical function for v_n^* was found which was independent of the type of blade, and which when used in calculations gave values of $i_{opt\infty}$ lying within permissible limits. In Fig.2 the empirical values of v_n^* so derived are plotted against stagger for various values of the pitch/chord ratio. The values of $i_{opt\infty}$ corresponding to this empirical function are plotted in Figs.3 and 4 for cambers of 25°, and 55°, and 85° and 115° respectively. It will be noticed that the scatter is within reasonable limits and quite random, there being no tendency for stagger or pitching to produce any systematic variation of $i_{opt\infty}$. The constant value assumed for each of these cambers has also been marked on these curves and in Fig.5 $i_{opt\infty}$ has been plotted against the camber angle (θ). It is thus possible to deduce from Figs.2 and 5 the optimum incidence for any cascade built up of the C.1 base profile on a circular arc camber line.

2.2 Deviation and Deflection

Knowing the optimum incidence (i_{opt}) it is only necessary to determine the deviation (δ) in order to completely relate the flow angles to the blade angles. Fortunately the deviation is only conditioned by Joukowski's hypothesis of stagnation at the trailing edge, a factor again dependent only on the potential flow round the aerofoil, and several well known rules^{9,19,20} have been formulated which readily give its value. The rule at present in use in N.G.T.E.²⁰ expresses the deviation as

$$\left. \begin{aligned} \delta &= m \theta \sqrt{s/c} && \text{for Compressor Cascades} \\ \delta &= m \theta s/c && \text{for Turbine Cascades} \end{aligned} \right\} \dots\dots\dots(6)$$

where m is a function of the position of maximum camber and stagger and has been plotted in Fig.6. As it stands this rule introduces a discontinuity between turbine and compressor cascades which does not exist in practise. Potential flow calculations would suggest a linear variation of deviation with pitch/chord ratio, for compressor as well as turbine cascades, while the test results would suggest a rule of the type

$$\delta = m \theta (s/c)^n \dots\dots\dots(7)$$

where m and n are both functions of the stagger. The discrepancy is probably due to three dimensional effects in the test results. In view of this and the inevitable large scatter of the test results it is considered more convenient to use the simple forms given in equation (6) rather than the more complicated one. Care should be taken in using these rules in border line cases, however. Once the deviation is known, and the optimum incidence determined as in section 2.1, the deflection, lift coefficient, loading factor etc., can easily be calculated.

3.0 The Performance at Optimum Incidence

The analysis so far described is sufficient to enable us to estimate the optimum conditions for any of the cascades of related aerofoils with which we are concerned. It tells us nothing, however, of the actual performance at that incidence, and how this is dependent on cascade geometry. Now it has been shown^{2,3} that the main criterion of the cascade performance is its loading factor (ψ). (Note. In ref.3 this was denoted by $CL(v_2)$ and designated "lift coefficient based on outlet velocity" - but see Section 1.0). The calculation of this factor is easy and straightforward but unfortunately it is not the complete criterion and several small corrections have to be applied before a suitable parameter can be determined. These corrections are considered independently in the next two sub-sections.

3.1 The Pitch/Chord - Thickness Correction

The pitch/chord - thickness effect is now well known, and need not be treated in any great detail here. As explained in ref.3 it is due mainly to the relatively smaller passage area encountered at closer pitching of the aerofoils. This gives rise to an increase in the drag coefficient, and a reduction in the loading factor as compared with their effective values at infinite pitch. Semi-empirical expressions have been derived connecting the actual values of these parameters with the corresponding value at infinite pitching, as follows:-

$$\psi_{\infty} = \psi \times \frac{6 s/c - 1}{6 s/c} \dots\dots\dots(8)$$

$$C_{Dp_{\infty}} = C_{Dp} \times \frac{6 s/c}{6 s/c - 1} \dots\dots\dots(9)$$

For the derivation of these equations the reader is referred to the original work (ref.3). These expressions will be used later but meanwhile it is necessary to examine a second correction to the simple ideas.

3.2 The Stagger Correction

According to the theory presented in ref.3 expressing all quantities relative to outlet conditions eliminates the differences between compressor and turbine cascades, and puts both on a common footing. This is not, however, strictly true, and it is rather interesting to examine the effect of changing the stagger on the performance at the optimum incidence, and to relate it with the type of performance at infinite pitch.

Let us consider a very simple case, and assume that we have an isolated aerofoil which has the idealised triangular pressure distribution shown in Fig.7. Now suppose that this aerofoil is employed in cascade. We can replace each of the aerofoils, except one by vortices as before, and since we are only dealing with the qualitative effect it will be sufficient to consider only the adjacent vortices. The cascades may then be represented by the systems shown in Fig.7. Although only two cases are considered here the series of cascades formed by a gradual change of stagger can all be represented and will in actual practise, form a gradual transition between each of the cases quoted.

Fig.7(a) shows the major velocity fields on the surface of any aerofoil due to the vortices representing the adjacent aerofoils of the cascade. In some cases it will be noticed that the induced velocity augments the basic velocity on the aerofoil surface, and consequently gives rise to a reduction of the local static pressure as at the points marked (1) and (4) in Fig.7. In other cases the induced velocity opposes the basic velocity and there is an increase in the local static pressure as at (2) and (3) in Fig.7. As a result of this velocity field the pressure distributions of the aerofoils in cascade will be modified as shown in Fig.7(b). In particular it will be noted that the compressor cascade will tend to have a "peaky" pressure distribution on the upper surface of each aerofoil, while the reaction turbine cascade will tend to have a more rounded distribution, with the peak suction well back from the leading edge of the aerofoil.

The low speed stalling characteristics for different types of pressure distributions have been discussed by Squire and Young²¹ and others. Generally speaking the peaky distribution is known to give a rapid stall, while the more rounded form of distribution gives a more gradual stall. The loss versus incidence curves for these examples will therefore take on the form shown in Fig.7(c). Furthermore, transition from a laminar to a turbulent boundary layer usually takes place just after the peak suction point, and so one would expect the compressor cascade to have a mainly turbulent boundary layer, and consequently a somewhat lower lift/drag ratio than the turbine cascade where quite a substantial portion of the boundary layer would be laminar. If, however, the pressure distribution should become too rounded, the boundary layer will not be able to negotiate the steep gradient near the trailing edge, and separation and high loss will ensue. The ideal case will be obtained, of course, when the boundary layer remains laminar over as large a portion of the aerofoil as possible but transition occurs immediately before the diffusion begins. The turbulent boundary layer should then just, but only just, be able to overcome the diffusion.

It must be emphasised that these notes represent a very simplified version of what actually occurs. The basic pressure distribution is always much more complicated than the simple triangular form assumed here, and the pitch/chord-thickness correction and the stagger correction should really be considered simultaneously. In spite of this the fundamental change in performance between the different types of cascades can easily be followed from simple vortex ideas. An example of the practical results is shown in Fig.8 where the exact pressure distribution (from potential flow calculations) and the test loss against incidence curves have been plotted for two representative types of cascade. It will be noted that they closely follow the simplified version cited above. The change in performance following a change in stagger is far too complex to permit a single quantitative correction factor as was possible in the case of the thickness - pitch/chord effect. Stagger (or outlet angle) will, therefore, have to be considered as one of the empirical parameters for evaluating cascade performance.

3.3 Scale Effect.

The fact that any type of pressure distribution, from the "low drag" to the "high lift" varieties, can be obtained on the same aerofoil by suitably choosing the stagger and pitch/chord ratio makes any generalisation on scale effect impossible. It is obvious that the critical Reynold's number will vary from cascade to cascade, and for practical applications the largely unknown turbulence factor make quantitative work even more difficult. For compressor cascades the critical Reynold's number appears to be somewhere between 1 and 2×10^5 , based on outlet velocity and chord. The critical Reynold's number for a compressor, however, appears to be only about one quarter of this value. This is probably due to wake interference and the high turbulence of the mainstream. With turbine cascades, on the other hand, we may well encounter large regions of laminar flow at quite high Reynold's numbers, and cascade tests on turbine blades do show marked scale effects. Similar observations have been made on turbines.

As stated in section 1.0 the effective Reynold's number, based on chord and outlet velocity was 3.5 to 4.5×10^5 for the test results used in the general analysis. This is above the critical value for compressor cascades and also just above the critical value of 3×10^5 for the turbine cascade test results of ref.22. Even so some of the phenomenally high efficiencies of some of the turbine cascades is probably due to a substantially laminar boundary layer at these Reynold's numbers. Some of the very low efficiencies may also be due to laminar flow, and early separation. Due allowance should be made for this when applying the results.

3.4 Performance Curves

Before dealing with the generalised performance curves it should be pointed out that it is more convenient when applying cascade results to compressors and turbines, to refer the performance to the fluid outlet angle, rather than the stagger angle; for the fluid angle is a measure of the swirl in the machine, and hence defines the type of characteristic that will be obtained.

Consider, then, the optimum performance of a series of cascades which all give the same fluid outlet angle. As the camber of the blades is increased the optimum lift coefficient will also increase. Likewise the lift/drag ratio will increase at first, but will reach a maximum and then start decreasing as the loading on the blades becomes excessive. In Figs.9, 10 and 11 the test values of the lift/drag ratio, modified to the corresponding value at infinite pitching by means of the relationships of section 3.1, have been plotted against the loading factor, also referred to infinite pitch. Separate plots have been presented for each of a series of fluid outlet angles, but many varied values of the test pitch/chord ratios have been used on each plot. Each of these has been denoted by a distinctive symbol. It will be noticed that the correction factors of section 3.1 have been sufficient to bring all the points close enough together to enable a single curve to be drawn through them for each fluid outlet angle. It will also be noticed that the scatter of the points is random, and no fundamental variation is apparently being ignored by this procedure. Assuming the curves drawn are representative, it is possible to construct a chart, as shown in Fig.12, in which the lines of constant lift/drag ratio have been plotted with the loading factor and fluid outlet angles as reference axes. Given any two of these quantities the third can then be determined. All values apply, of course, to infinite pitching, and must be corrected to the required pitch/chord ratio by the usual method. This has been done in Figs.13, 14 and 15, for pitch/chord ratios of 0.5, 1.0 and 1.5 respectively. Plotted in this way it is believed that the curves convey more than the unique relationship of Fig.12, but interpolation for other pitch/chord ratios is carried out more easily from the original chart.

An examination of the general shape of the contours in Fig.12 is rather interesting, and checks up with the comments of section 3.2 remarkably well. It will be noticed that the peak value of the efficiency or lift/drag ratio, increases towards the turbine region, reaching a maximum at a fluid outlet angle of about -40° . For fluid angles less than about -50° the efficiency falls off very rapidly, due to the steep gradient at the trailing edge associated with very convex pressure distributions. The upper limit of efficiency is due, of course, to the excessive loading of the blade and the consequent breakaway, but the lower limit is due to a low work capacity rather than to any very marked increase in drag. Some further remarks regarding these contours are made in the general comments on the analysis at the end of the report (section 6.0).

4.0 Performance at Other Incidences

Next to the optimum incidence the most important point on the characteristic is the stalling incidence. It is self evident that stalling is due to a certain increase of loading above the optimum, and that the incidence increment is a suitable measure of this. Furthermore it would seem reasonable to suggest that the effective loading factor at the optimum incidence

will be a good criterion of the additional load that can be borne by the aerofoils before they stall. In Figs.16, 17 and 18, therefore, the incidence increment between optimum and stalling incidence has been plotted against the effective loading factor for various values of the outlet angle: The scatter of the points on some of these plots is considerable. This may, in part, be due to an inadequate definition of stalling (see section 1.0) but is also probably largely due to the fact that stalling is an unstable process, for which no exact quantitative analysis is possible. The scatter was quite random, neither of the various variables exerting any definite trend on the results, so straight lines were drawn through the points as representing the best mean values. From these lines the general chart of Fig.19 was prepared, which gives the incidence increment at stalling for all values of the loading factor and fluid outlet angle. The general tendency for the incidence increment to increase towards the turbine region is again in accordance with the general ideas presented in section 3.2.

Once the optimum and stalling incidence is known, the characteristic is virtually determined, the exact variation of loss between these two points being largely immaterial. Quite a good approximation to the actual curve could be drawn in from experience, but as a guide Fig.20 shows the type of variation to be expected between these two points. It has been derived on the assumption that all loss and deflection against incidence curves are geometrically similar and mean values taken. It is considered that this curve is sufficiently accurate for most practical purposes.

No attempt has been made to estimate the negative stalling incidence of this series of cascades. No reliable parameter has yet been found and further work is necessary before a suitable method can be evolved.

The curves given in Figs.2, 5, 12, 19 and 20 are, however, sufficient to provide the most important portion of the low speed performance characteristic of any cascade of blades having the C.1, C.2 or C.4 base profile on circular arc camber lines. An example of the calculation of a sample characteristic is given in Appendix II

5.0 The Effect of Modifications to the Profile

In the preceding analysis we have been concerned only with the series of cascades formed by superimposing the C.1 base profile on circular arc camber lines. Very often other profiles have to be used, and so in this section we shall examine, very briefly, the changes in performance to be expected from any change in the profile. Provided a good contour is maintained test evidence would suggest that small alterations to the aerofoil profile will have little effect on the overall performance. This leaves only the major variables which can be enumerated as follows:-

- (1) Leading Edge Radius.
- (2) Trailing Edge Thickness.
- (3) The Maximum Thickness.
- (4) The Position of the Maximum Thickness.
- (5) The Position of the Maximum Camber.

Of these the first two are of minor importance at low speeds provided they lie within the normal range. The leading edge radius may be expected to affect the performance, but it would seem that a good form is of more importance than anything else. At high speeds the leading edge contour is probably far more critical.

Trailing edge thicknesses up to 20% of the maximum thickness appear to have little effect, and as this should be well within manufacturing tolerances little further need be done about this feature. The remaining three variables do, however, appear to have a more substantial effect on the performance, and are considered separately in the next two sub-sections.

5.1 Maximum Thickness

In connection with this item we have to consider as noted above, both the position of the maximum thickness along the chord, and also its value. Very little information exists regarding the former, a single test (ref.11) and some very little theoretical work (ref.20) being all available. Both these sources of information agree however that moving the position of maximum thickness back towards the trailing edge is bad for the low speed performance. While not changing the optimum performance to any noticeable extent it considerably reduces the working range. Any advantages that may arise from changing the position of maximum thickness will appear at high speeds only, and some compromise may be necessary on this account.

A little more information does exist concerning the effect of variations in the magnitude of the maximum thickness. It is, however, very scattered and not altogether conclusive. According to the ideas of ref.3, recapitulated in Section 3.1, the pitch/chord - thickness correction implies a better performance for thinner blades on account of the relatively larger passage area. This has received some support from tests on sheet metal blades for corners²⁾ where they are shown to be better than faired sections. They are of course, only working at a fixed incidence, which can be suitably adjusted. Complete cascade tests, however, show that while the loss through the cascade is reduced by the use of thinner sections, so too is the maximum permissible blade loading. The reduction in the optimum loading factor may be quite large, as shown for instance in Fig.21(a), where the loading factor and the lift/drag ratio have been plotted against maximum blade thickness. It will be noticed that the efficiency is roughly constant for the thinner sections but falls off rapidly with increase of thickness chord ratio much above 10%. At high speeds Mach No. effects accentuate this tendency. Some Reynold's Number effects are suspected in the tests quoted but they do lay emphasis on the fact that care should be taken in using sections whose maximum thickness varies greatly from conventional values, particularly if they are thick sections.

5.2 The Position of Maximum Camber

Rather more information is available on the effect of moving the position of maximum camber. The work of the Stear Nozzle Research Committee (ref.24) contains much that is of a relevant nature in the turbine range, while the theoretical work of ref.20 and the test results of refs.11, 25, 26 give a good deal of information on compressor cascades. If any generalisation is possible it would be to the effect that moving the position of maximum camber forward tends to produce higher velocities, or lower pressures, near the leading edge on the upper surface of the aerofoil. This is due, of course to the greater curvature in that region with that type of aerofoil. It will be remembered from section 3.2 that increasing the fluid outlet angle also produced higher velocities near the leading edge on the upper surface. Moving the position of maximum camber forward can thus be regarded for qualitative purposes as equivalent to operating at a higher fluid outlet angle. For example, with the so-called parabolic blading (i.e. position of maximum camber 40% chord from the leading edge) the contours on Fig.12 would be moved to the left with respect to the fluid outlet scale. This type of aerofoil is often used and it would have been desirable to have the lift/drag contours for it corresponding to Fig.12 for circular arc camber lines. Unfortunately not sufficient results were available to determine the curves adequately, and so a certain amount of "intelligent anticipation" will have to be used in design work. From the results that were available, however, it was possible to produce a tentative curve of $i_{opt_{\infty}}$ against camber angle (θ), and this has been shown dotted in Fig.5. The empirical function for v_n^* used for circular arc camber lines appears to be equally satisfactory for parabolic camber lines. A series of tests is at present being carried out at N.G.T.E. on aerofoils with parabolic camber lines, and from the results the efficiency contours will be determined accurately.

The different types of pressure distributions obtained from the various positions of the point of maximum camber can be used to counteract any undesirable features in the distribution that may occur at some fluid outlet angles. Combinations of the position of maximum camber and the fluid outlet angle together with the resulting upper surface pressure distribution are shown in Fig. 22. If a more or less constant distribution without any steep gradient is wanted and this would appear generally desirable, one would expect the position of maximum camber to be well forward for low fluid outlet angles and further back for high fluid outlet angles. This avoids steep gradients at the trailing edge with turbine cascades and excessive peakiness with compressor cascades, as shown in the figure. It has been known for some time^{2,4} that plenty of curvature near the leading edge is desirable for turbine nozzles, and recently the advantages of reducing this curvature for compressor cascades has been appreciated. The intermediate types of cascades can be expected to fall in between these two extremes, and in Fig. 21(b) a very tentative curve has been drawn showing the variation of the position of maximum camber with fluid outlet angle. The normal recommended point derived from some unpublished results and a point derived from the results given in ref. 24 have been taken as the basic points on this curve, but the actual value of the second point must be regarded with suspicion. It is interesting to note how the conventional type of turbine blade design (i.e. circular arc and straight line construction) seems to fall in with the general shape of the curve.

These remarks on profile modifications are necessarily sketchy as test information is almost non-existent. An attempt has been made, however, to note the general tendencies that will have to be observed when designing cascades of such blades. These tendencies should be borne in mind when considering the general notes of the next section, which apply to the standard related series used for the main analysis.

6.0 Some General Comments

It is very difficult, if not impossible, to produce design data which will have universal application, and each particular case should be considered on its own merits. In most cases, however, the desirable features will be a high efficiency, and a high work capacity. The highest efficiency for any type of cascade can be obtained with a design located on the top of the "ridge" of contours in Fig. 12. There will always be a tendency, however, to sacrifice some efficiency for a high work capacity, i.e. to work slightly below the top of the ridge on the high load side. While this may be quite suitable for certain applications, the dangers of such a practice should be noted. The reduction of efficiency at high loading is due to incipient breakaway, and this implies a rather unstable state of the boundary layer on the upper surface of the aerofoil. Standards of aerofoil surface finish can therefore be expected to have a marked influence on the amount of breakaway that occurs in such circumstances. A fairly high standard of manufacture was maintained for all the aerofoils whose test results were used in the general analysis of this report, so any signs of an efficiency curve falling with increased loading must be regarded as a danger sign. Poor blade manufacture may well produce disturbances that will convert incipient into complete breakaway. In this case the actual performance will be considerably worse than that given by the general curves.

It should also be noted that overloading is more dangerous with a concave pressure distribution than with a convex, because most of the boundary layer will be near the separation point, and any disturbance will cause the breakaway to occur well forward with a marked reduction in efficiency. Breakaway is only likely to occur near the trailing edge with a convex distribution, however, and the loss in efficiency will not then be so great.

An example of what is likely to occur in practice is shown in Fig. 23. In this figure the salient performance parameters have been plotted against blade camber for cascades having a pitch/chord ratio of unity and giving a fluid outlet angle of 20° . The curves in this figure have been derived from the general curves given earlier in this report. Although definite curves have been drawn, it can easily be appreciated that above cambers of about $35 - 40^\circ$, where the drag is beginning to increase rapidly, no guarantee of performance can be made. This is well illustrated by the nominal deflection

curve, for also plotted in Fig.23 is the equivalent 'nominal' deflection curve derived from some unpublished low speed results obtained from No.2 High Speed Cascade Tunnel. The blade chord was only $\frac{1}{2}$ " in these tests, and so the accuracy of manufacture necessarily suffered a little and this is probably the cause for the difference in deflection for cambers above $35 - 40^\circ$ obtained from this tunnel as compared with the calculated values. The corresponding drags were not measured in No.2 tunnel and so a comparison of these cannot be made, but they would probably be much higher than calculated from the general curves. The necessity for keeping well away from this danger zone unless conditions are closely controlled is clearly illustrated by these results.

The calculation of the appropriate camber, stagger, and pitch/chord ratio required to fulfil any given duty is rather tedious though quite straightforward. A set of charts, giving similar information to that presented in Fig.23, has therefore been prepared. These cover a wide range of outlet angle and pitch/chord ratio, and will be issued in a separate note.

To give some guide to the correlation between the results of this analysis and the test results obtained in other tunnels the following table compares the calculated values with some test values that were obtained recently and which were not used in the analysis.

Cascade Details

Source	Aerofoil	ζ	s/c	i_{opt}	α_2	$(L/D)_{max}$	i_{stall}	
Ref.25	10C4/25C50	-42.5°	0.75	(Test	$+5.0^\circ$	36.0	47	$+10.7^\circ$
				(Calc.	$+4.0^\circ$	36.5°	47	$+ 8.9^\circ$
	10C4/25P40	-37.6	0.75	(Test	0.0°	34.5°	48	$+ 6.5^\circ$
				(Calc.	$+0.8^\circ$	34.8°		
	10C1/40C50	-24.6	1.0	(Test	-1.0	15.7°	45	$+ 4.5^\circ$
				(Calc.	-3.6	14.7°	62	$+ 3.3^\circ$

The complete calculated and test characteristics for the two cascades of circular arc blades are given in Figs.24 and 25. It will be seen that the results from these differing sources are substantially in agreement with the calculated values. Small differences that do exist can be attributed to tunnel effects (or possibly to some Reynold's number effects though this is unlikely). For instance in Fig.26 the calculated and test characteristics have been compared for a cascade of 10C1/40C50 aerofoils at a stagger of -27.5° and a pitch/chord ratio of 0.94. The test results were taken from ref.9 and were used in the analysis. Agreement is very good and somewhat better than that obtained with the results from No.6 High Speed Tunnel (Fig.25) although the cascades were very similar.

Finally it should be mentioned that it was rather unfortunate that the series of aerofoils we have taken for the general analysis is not really representative of turbine practise. For the reasons given in section 5.2 it would be impossible to pick a series ideally suitable for both compressors and turbines, and the choice in this particular case was greatly influenced by the amount of test information available. It is anticipated that a similar analysis could be carried out for more suitable sections when sufficient test data has been accumulated.

7.0. Conclusions

It has been shown in this report that a general analysis of cascade information is possible, and that this analysis can be applied to turbine and

compressor cascades alike. An attempt has been made to explain the behaviour of various types of cascades and data is given from which any cascade of aerofoils having the C.1, C.2 or C.4 base profile on circular arc camber lines can easily be calculated. Appreciating the fundamental factors involved it should be possible to make a close estimate of the performance of other sections, and so to gain some idea as to what improvements can and cannot be made.

REFERENCES

<u>No.</u>	<u>Author</u>	<u>Title</u>
1.	A. R. Howell, M. Mettam and J. Nock.	"Some General Notes on Axial Flow Compressor Design". A.R.C. 9160. May, 1945. (unpublished)
2.	O. Zweifel.	"The Spacing of Turbo-machine Blading, especially with Large Angular Deflection" Brown Boveri Review Vol. XXXII No. 12. Dec. 1945.
3.	A. R. Howell and A. D. S. Carter.	"Fluid Flow through Cascades of Aerofoils" Sixth International Congress for Applied Mechanics. Paris. Sept. 1946. A.R.C. 11,173.
4.	A. Betz	"Diagramme zur Berechnung von Flugelreihen". Ingenieur Archiv. 2 page 359 (1931) Available as N.A.C.A. Technical Memorandum No. 1022 (1942).
5.	E. Pistolesi	"Sul calcolo di schiere infinite di ali sottili" Pubblicazioni della R. Scuola d'Ingegneria di Pisa (7 series) No. 323 (Sept. 1937). English Translation available as N.A.C.A. Tech. Memo. No. 968 (1941).
6.	J. Ackeret	"Zum Entwurf dichtstehender Scharfeligitter" Schweiz. Bauztg. 120 Heft 9 (1942) English Version available in R.T.P. Translation No. 2007.
7.	S. Katzoff, Robert S. Finn and James C. Lawrence.	"Interference Method for Obtaining the Potential Flow past an Arbitrary Cascade of Airfoils". N.A.C.A. Technical Note No. 1252 (May 1947.)
8.	L. Diesendruck	"Iterative Interference Methods in the Design of Thin Cascade Blades" N.A.C.A. Technical Note No. 1254 (May 1947).
9.	H. Constant	"Performance of Cascades of Aerofoils" R.A.E. Note No. E.3696 A.R.C. 4155. 1939. (unpublished)
10.	J. Reeman	"Note on Positive Stagger Cascades" R.A.E. Tech. Note No. Eng. 202 (1943).
11.	A. R. Howell	"A Note of the Compressor Base Aerofoils C.1, C.2, C.3, C.4 and C.5, and Aerofoils made up of Circular Arcs", Power Jets (R & D) Ltd., Memorandum No. M.1011 (1944).
12.	A. R. Howell	"The Fluid Dynamic of Axial Compressors". Proc. I. Mech. E. Vol. 153 p. 441 (1945).

13. J. Reeman. "The Performance of Cascades of Aerofoils at Positive Stagger" A.R.C. 10,829. 1946. (unpublished).
14. R. G. Harris and R. A. Fairthorne. "Wind Tunnel Experiments with Infinite Cascades of Aerofoils" R & M 1206 (1928).
15. K. Christian. "Experimentelle Untersuchung eines Tragflugel-profiles bei Getteranordnung" Luftfahrtforschung Vol.II (1928).
16. C. Keller. "Axialgebläse von standpinkt der Tragflugel-theorie" Institute fur Aerodynamik Zurich (1934). Part available as an A. II. Translation ref. Ae Techl.1013, A.P.135 (1935). A.R.C.2161.
17. Y. Shinoyama. "Experiments on Rows of Aerofoils for Retarded Flow" Memoirs of Faculty of Engineering - Kyushu Imperial University, Fukuoka, Japan. Vol.III No.4 (1938).
18. A. R. Howell. "The Present Basis of Axial Compressor Design Part I - Cascade Theory - Performance" R & M 2095 (1942).
19. J. Wrigley and J. T. Hansford. "Flow of an Ideal Fluid Past a Cascade of Blades" Metropolitan-Vickers Report (1944).
20. A. D. S. Carter and H. P. Hughes. "The effect of Profile Shape on the Performance of Aerofoils in Cascade" R & M 2384 (1946).
21. H. B. Squire and A. D. Young. "Wing Sections and their Stalling Characteristics" Appendix to R. A. E. Report No. Aero 1718 (1942).
22. E. A. Bridle. "Some High Speed Tests on Turbine Cascades" R & M. 2697. February, 1949.
23. K. G. Winter. "Comparative Tests on Thick and Thin Turning Vanes in the 4 ft x 3 ft Wind Tunnel" R. & M. 2589. August, 1947.
24. Steam Nozzles Research Committee. Fourth Report of the Steam Nozzles Research Committee Proc.I. Mech. E. No.4 1925.
25. S. J. Andrews. "A comparison between Two Compressor Cascades using C.4 profile on Parabolic and Circular Arc Camber Lines" A.R.C. 10,269. (1946).

APPENDIX I

Notation

a	distance of point of maximum camber from L.E.
b	maximum camber.
c	chord.
i	incidence.
r_1	radius of curvature at L.E.
r_2	radius of curvature at T.E.
s	blade spacing or pitch.
t	blade maximum thickness.
C_D	drag coefficient.
C_L	lift coefficient.
C_{Lth}	theoretical lift coefficient.
L.E.	leading edge.
M_n	Mach Number.
P	static pressure.
P_{tot}	total head pressure.
R_n	Reynold's Number.
T.	static temperature.
T_{tot}	total head temperature.
T.E.	trailing edge.
T.F.	turbulence factor
V	velocity, V_a V_m V_w are axial, vector mean, and whirl velocities respectively.
α	air angle
α^*	nominal fluid angle.
α_{opt}	optimum fluid angle.
α_m	vector mean fluid angle.
β	blade angle.
δ	deviation.
ζ	stagger.
θ	camber.
x_1	camber inlet angle.
x_2	camber outlet angle.

- ψ loading factor.
- w loss of total head.
- ΔP local static pressure minus free stream static pressure.
- * denotes nominal conditions (see Section 2.1).

Suffices

- m vector mean values.
- opt optimum values (see section 2.1).
- 1 inlet to cascade.
- 2 outlet from cascade.

Aerofoil Nomenclature

The nomenclature defining the aerofoil is best illustrated by the example

1001/40050

Here 10 denotes the maximum thickness (t) in % chord; 01 denotes the base profile; 40 is the camber angle (θ) in degrees; C denotes a circular arc camber line and 50 the position of maximum camber (a) in % chord from the leading edge. The two forms of camber line normally used are circular arc (denoted by C) and parabolic arc (denoted by P).

To construct the aerofoil the ordinates of the base profile are multiplied by the ratio of required maximum thickness divided by the base aerofoil maximum thickness and are then plotted normal to the chosen camber line, stations being taken along the camber line itself.

APPENDIX II

The Calculation of Cascade Characteristics

As an example consider the calculation of the characteristic for the following cascade -

Aerofoil 1004/25050

Stagger -42.5°

Pitch/Chord Ratio 0.75

Blade inlet angle (β_1) = 55°

Blade outlet angle (β_2) = 30°

The deviation $\delta = m\theta/\sqrt{s/c} = 0.30 \times 25 \times \sqrt{0.75} = 6.5^\circ$

where m is obtained from Fig 6

Fluid outlet angle (α_2) = $\beta_2 + \delta = 36.5^\circ$

The calculation of the optimum incidence cannot be done directly and a method of successive approximations will have to be used. For most cascades in general use it will be found convenient to assume $i_{opt} = 0^\circ$ as a first approximation.

1st Approximation $i_{opt} = 0^\circ$

$$\left. \begin{aligned} \alpha_{1opt} &= 55^\circ \\ \alpha_2 &= 36.5^\circ \end{aligned} \right\} \epsilon = 18.5^\circ \text{ and } C_L = 0.697$$

$$\begin{aligned} \Delta_1 &= \frac{v_n^* \times C_L}{2 \times s/c} \times 57.3^\circ \\ &= \frac{0.207 \times 0.697}{2 \times 0.75} \times 57.3^\circ = 5.5^\circ \end{aligned}$$

where the value of v_n^* has been taken from Fig 2 for the given values of stagger and pitch/chord ratio. But $i_{opt\infty}$ for $\theta = 25^\circ = -2.8^\circ$ from Fig 5 whence $i_{opt} = +2.7^\circ$ as compared with an assumed value of 0° . Using this value of i_{opt} a second approximation can be found and so on. A certain amount of "anticipation" reduces the number of approximations necessary. It is readily seen that increasing i_{opt} increases C_L and hence Δ_1 . But $i_{opt\infty}$ remains constant for the blade. Hence let us take a slightly higher value of i_{opt} for the second approximation = 4.0° say.

2nd Approximation $i_{opt} = 4.0^\circ$

$$\left. \begin{aligned} \alpha_{1opt} &= 59.0 \\ \alpha_2 &= 36.5 \end{aligned} \right\} \epsilon = 22.5^\circ \text{ and } C_L = 0.885$$

whence $\Delta_1 = 6.8^\circ$

and $i_{opt} = 6.8 - 2.8 = \underline{4.0^\circ}$

∴ Optimum Conditions are

$$\text{Fluid Inlet Angle } \alpha_1 = 59.0^\circ$$

$$\text{Fluid Outlet Angle } \alpha_2 = 36.5^\circ$$

$$\text{The loading factor } (\psi) = 1.39$$

$$\text{Therefore } \psi_\infty = \psi \times \frac{6 \text{ s/c}}{6 \text{ s/c} - 1} = 1.79$$

$$\text{whence } (L/D)_\infty = 77 \text{ (from Fig.12)}$$

$$\text{and } i_{\text{stall}} - i_{\text{opt}} = 4.9^\circ \text{ (from Fig.19)}$$

$$\text{so that we get } \left[\frac{L}{D} \right]_{\text{max}} = \left[\frac{L}{D} \right]_\infty \times \left\{ \frac{6 \text{ s/c} - 1}{6 \text{ s/c}} \right\}^2 = 47$$

$$\text{giving } C_D = \frac{C_L/L}{\Gamma} = \frac{0.885}{47} = 0.0188$$

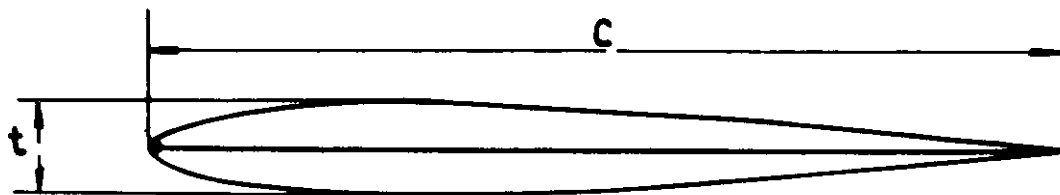
$$\text{or } w/\frac{1}{2}\rho V_1^2 = \frac{C_D}{\text{s/c}} \times \frac{\cos^2 \alpha_1}{\cos^3 \alpha_m} = 0.0254$$

$$\underline{0.025}$$

$$\begin{aligned} \text{and } i_{\text{stall}} &= i_{\text{opt}} + (i_{\text{stall}} - i_{\text{opt}}) = +4.0^\circ + 4.9^\circ \\ &= \underline{+8.9^\circ} \end{aligned}$$

From these values the full characteristic, geometrically similar to the curves of Fig.20 can be drawn as shown in Fig.25.

(a) BASE AEROFOIL C. I.



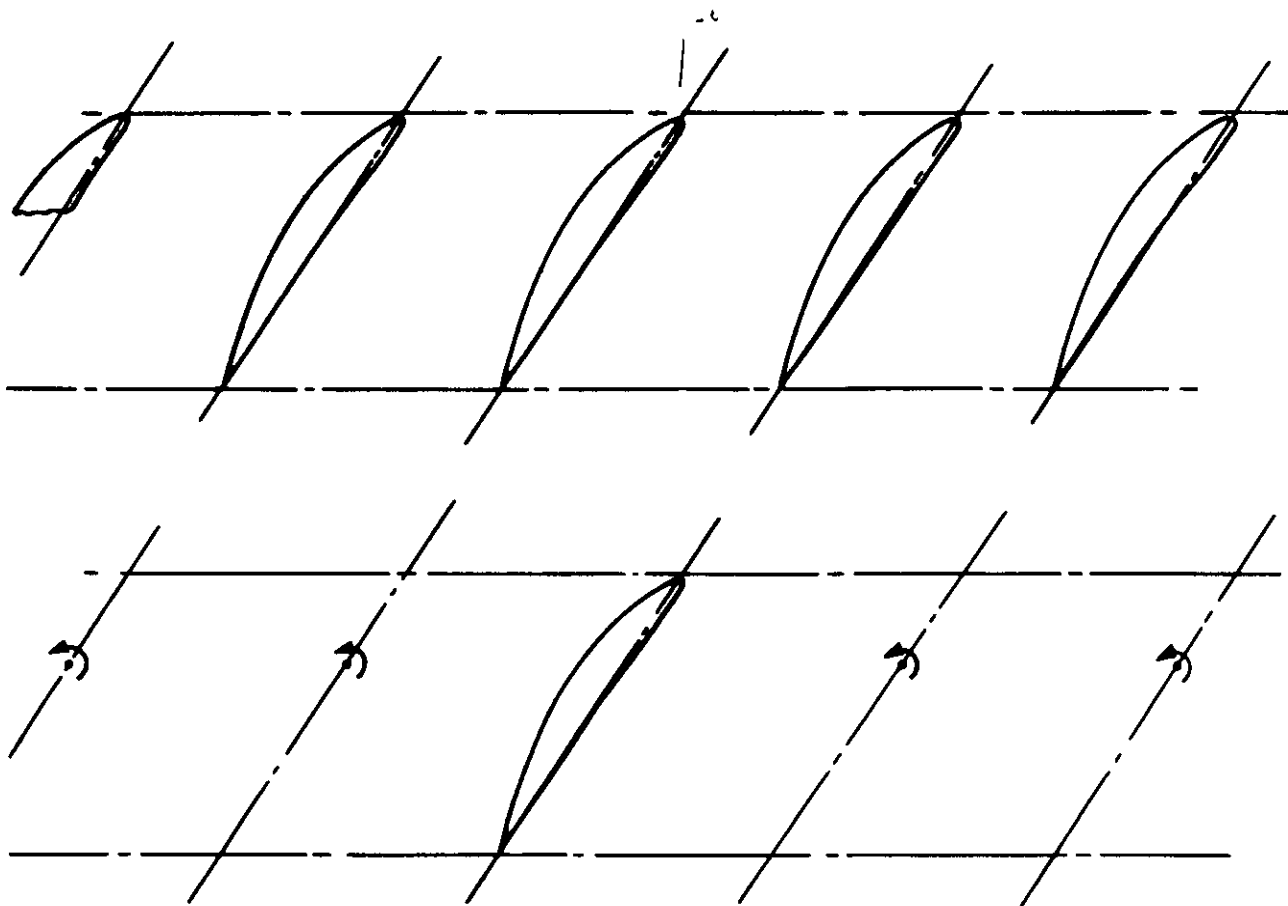
LE RAD = 8% t t/c = 10% TE. RAD = 2% t

STATION	0	1.25	2.5	5.0	7.5	10	15	20	30	40	50	60	70	80	90	95	100
UP'R & LW'R	0	4.375	1.94	2.675	3.225	3.6	4.175	4.55	4.95	4.81	4.37	3.75	2.93	2.05	1.125	0.65	0

} % OF C

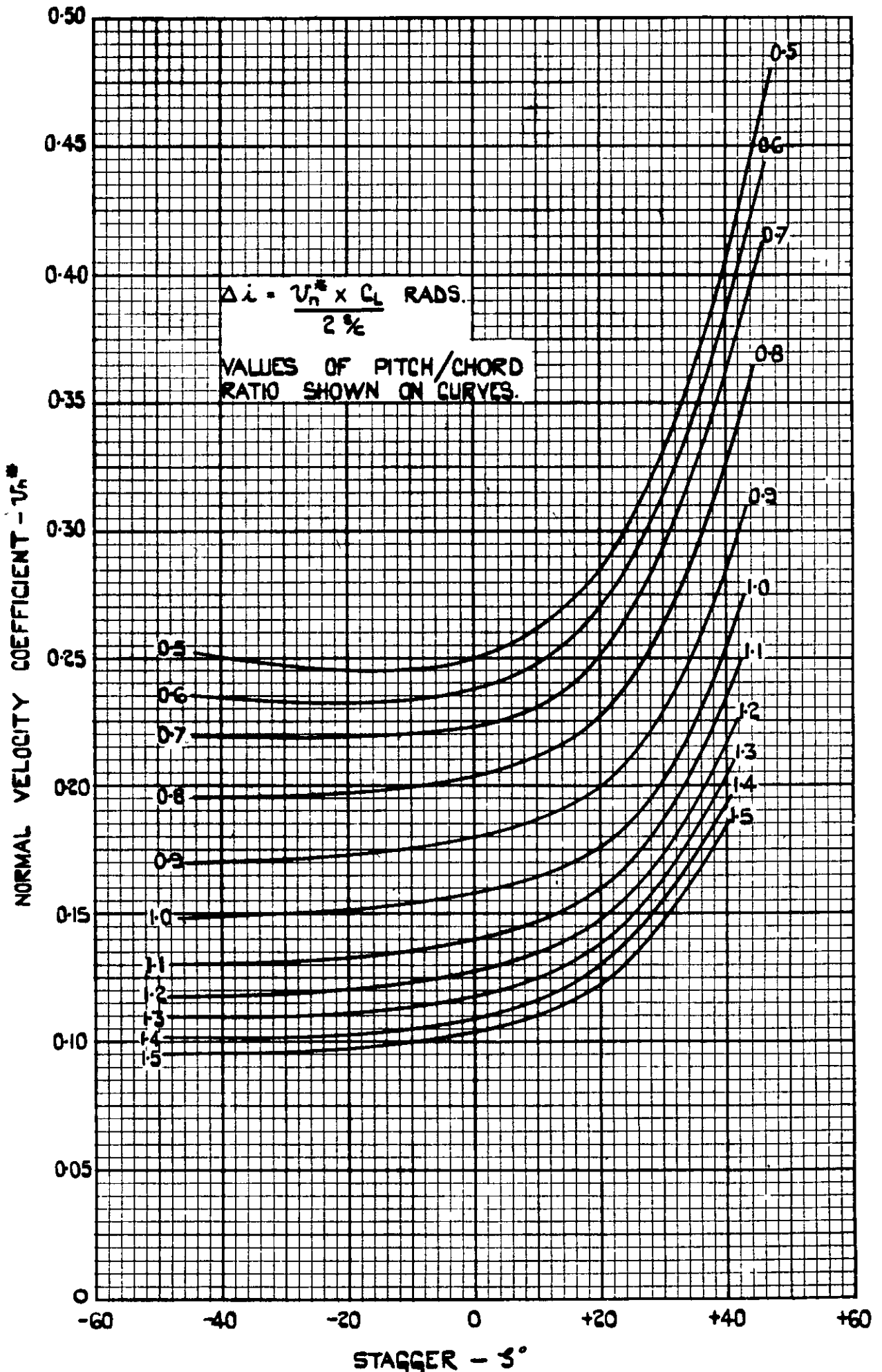
STATION OF MAX THICKNESS = 33% OF C.

(b) VORTEX REPRESENTATION OF CASCADE.

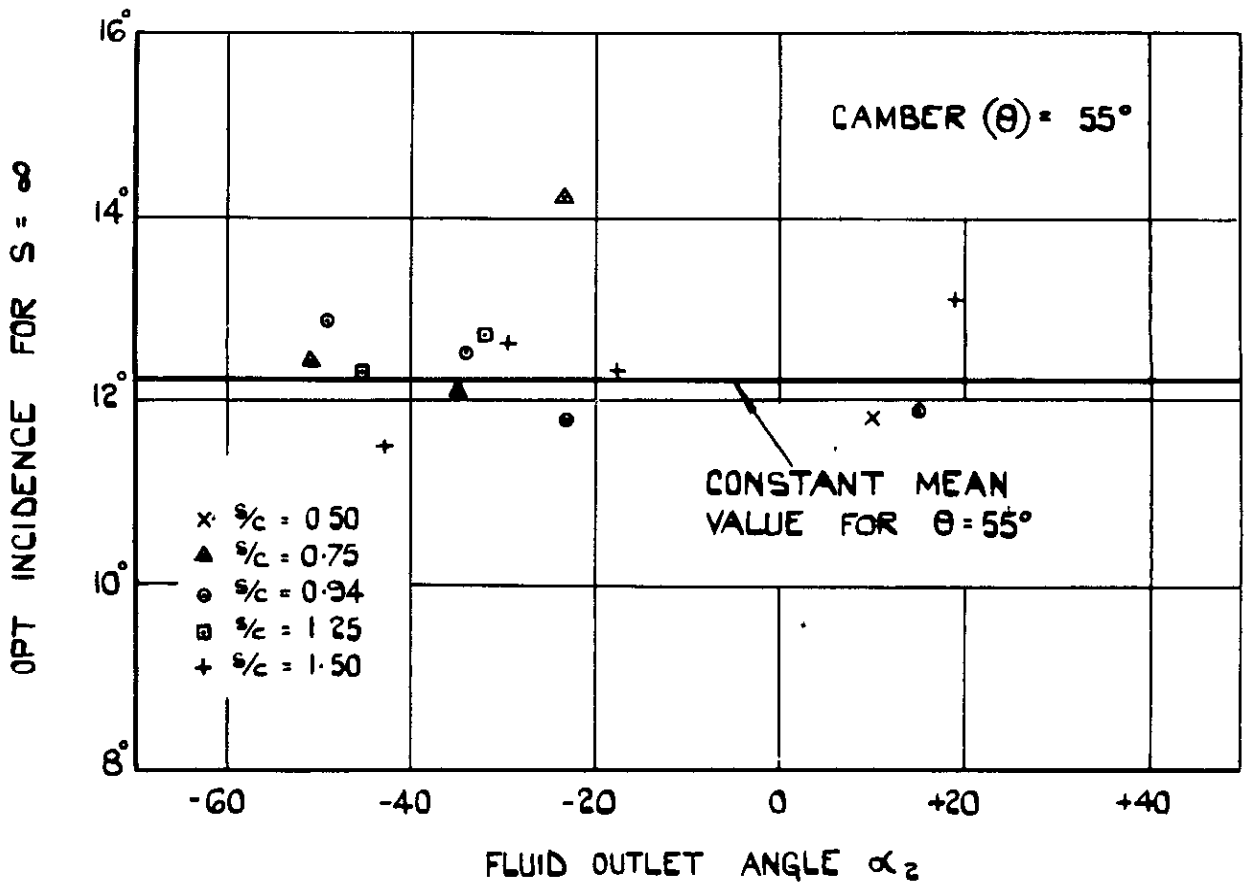
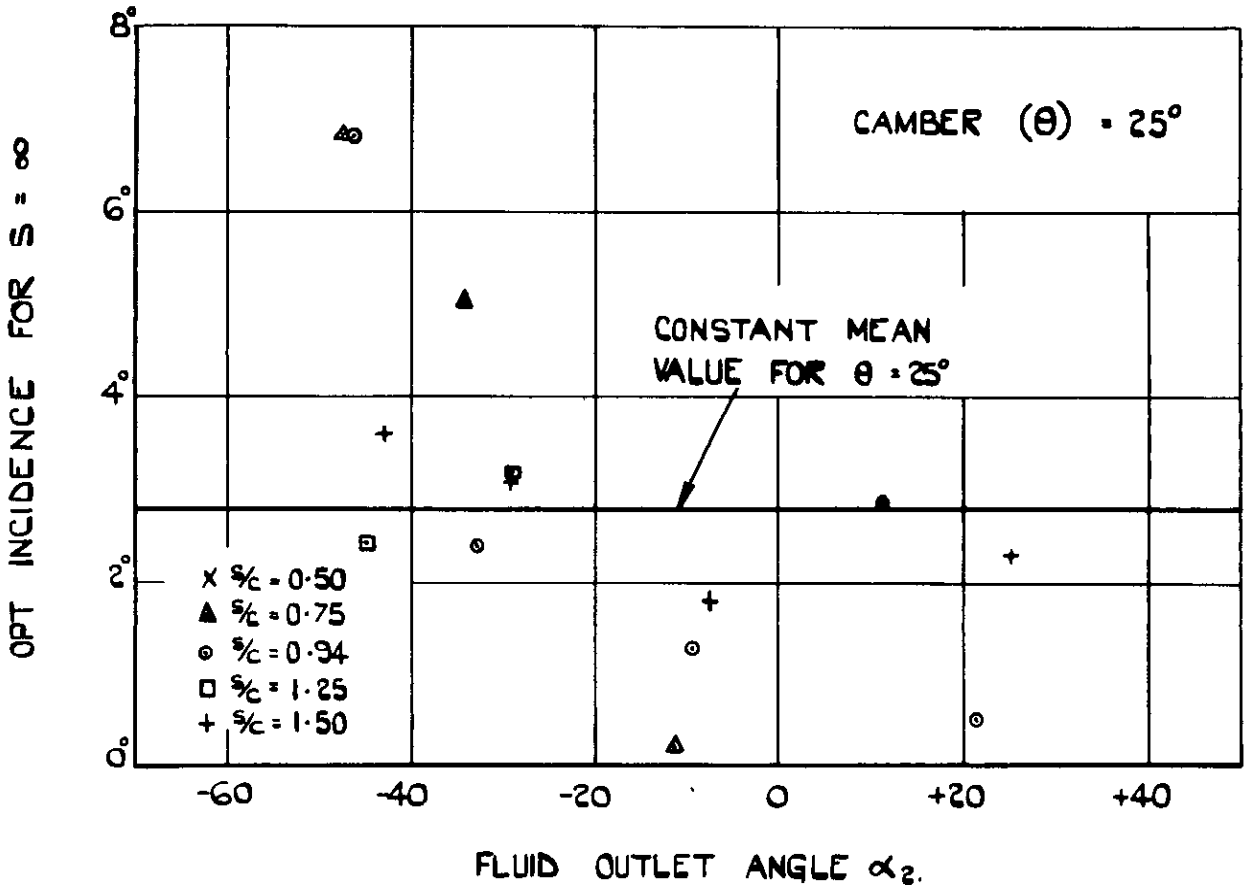


RESTRICTED

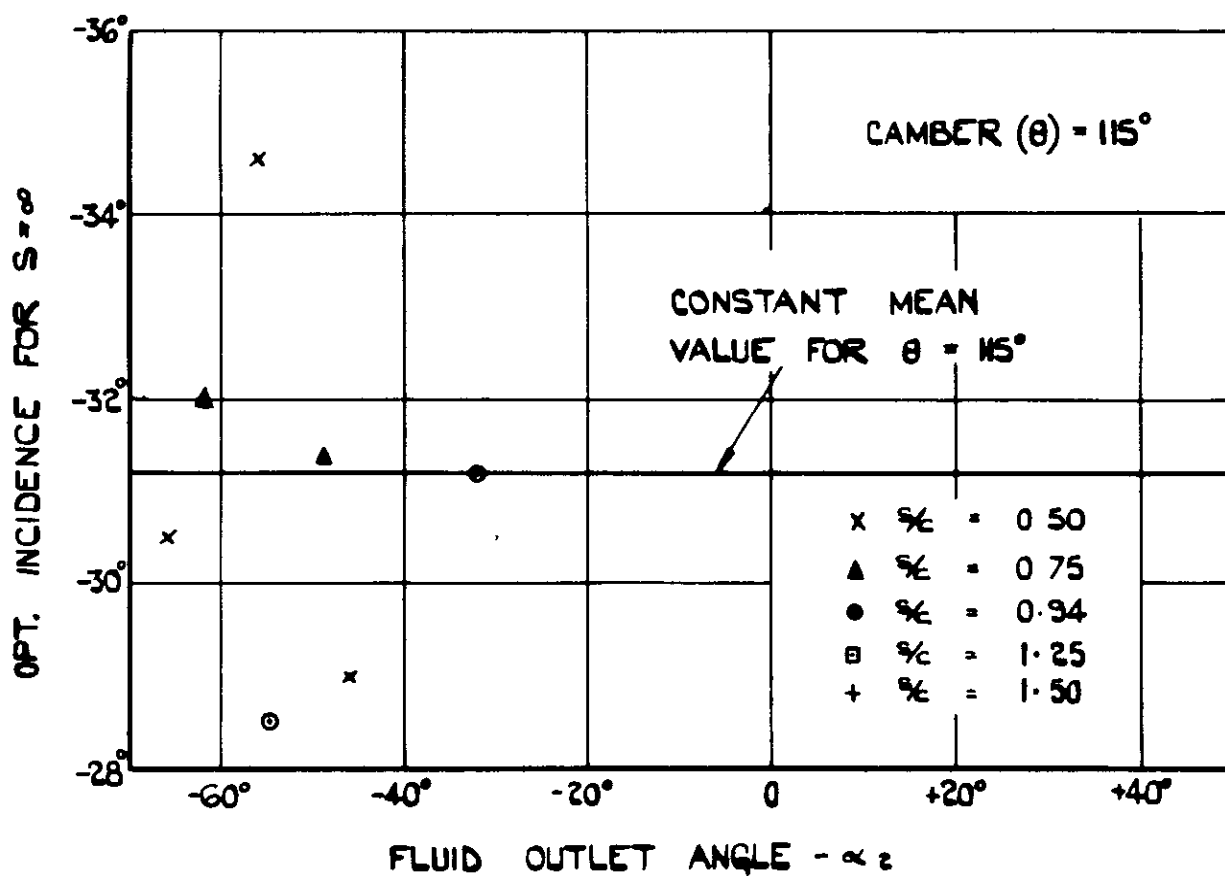
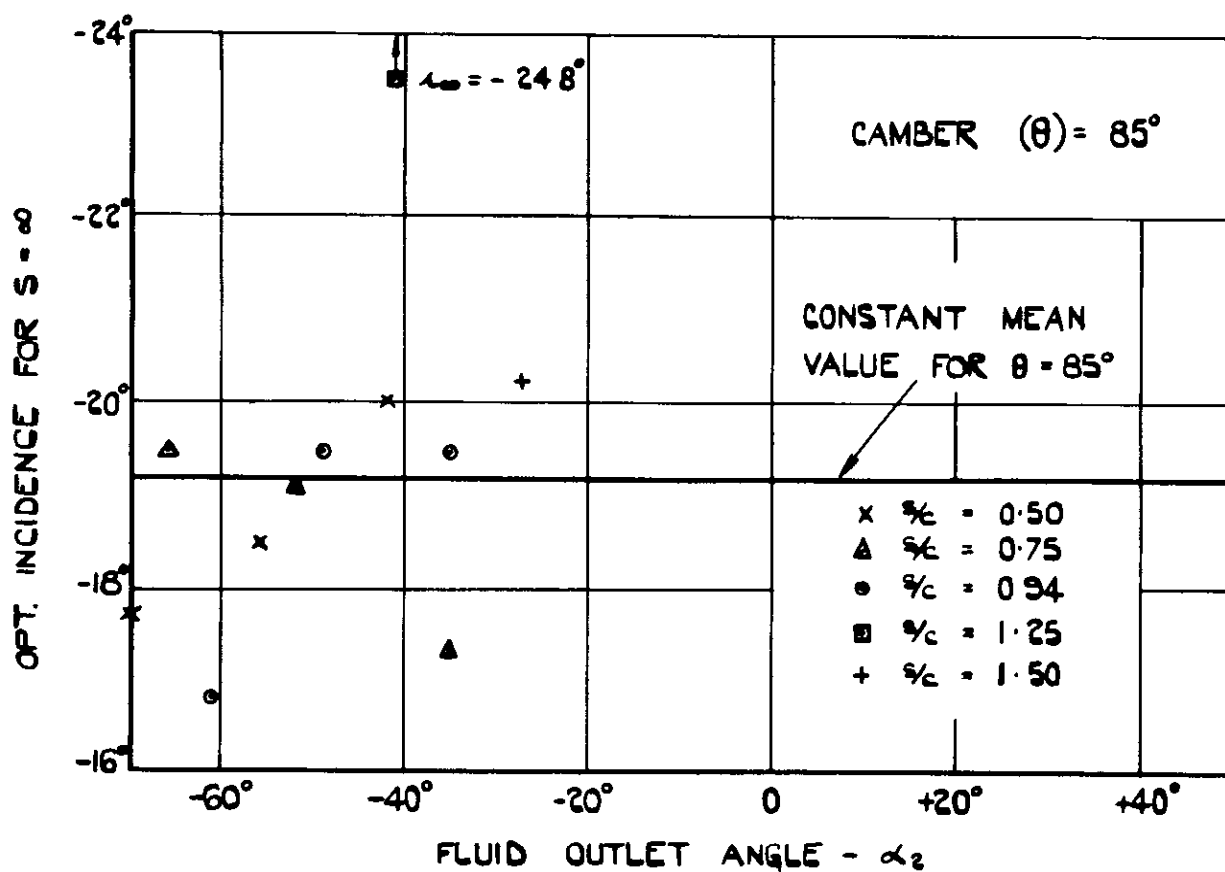
NORMAL VELOCITY COEFFICIENT.



VALUES OF $i_{OPT\infty}$ FOR VARIOUS CAMBERS.



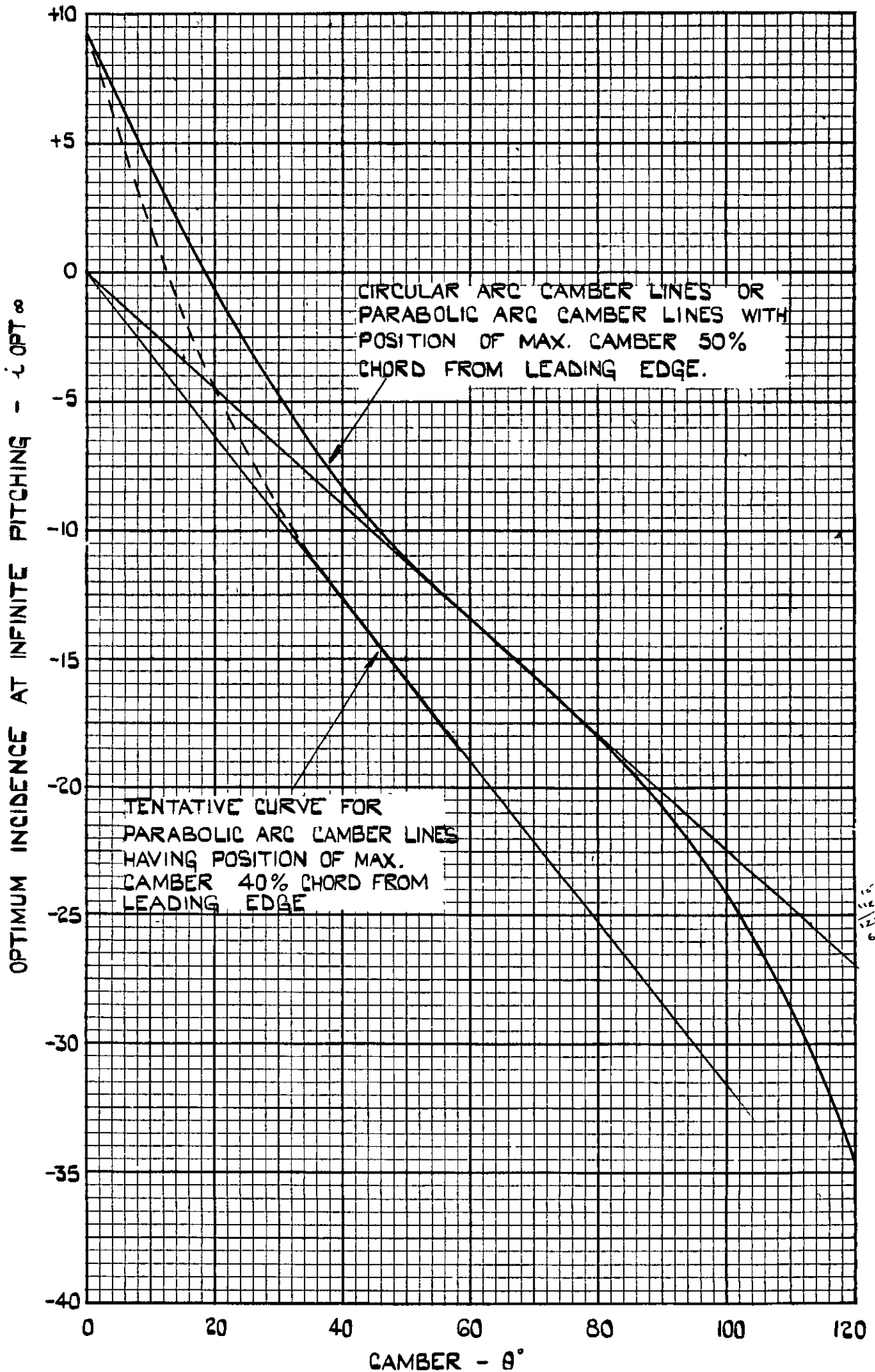
VALUES OF $\lambda_{OPT\infty}$ FOR VARIOUS CAMBERS.



OPTIMUM INCIDENCE AT INFINITE PITCHING.

(MEAN VALUES TAKEN FROM FIGS 3 & 4.)

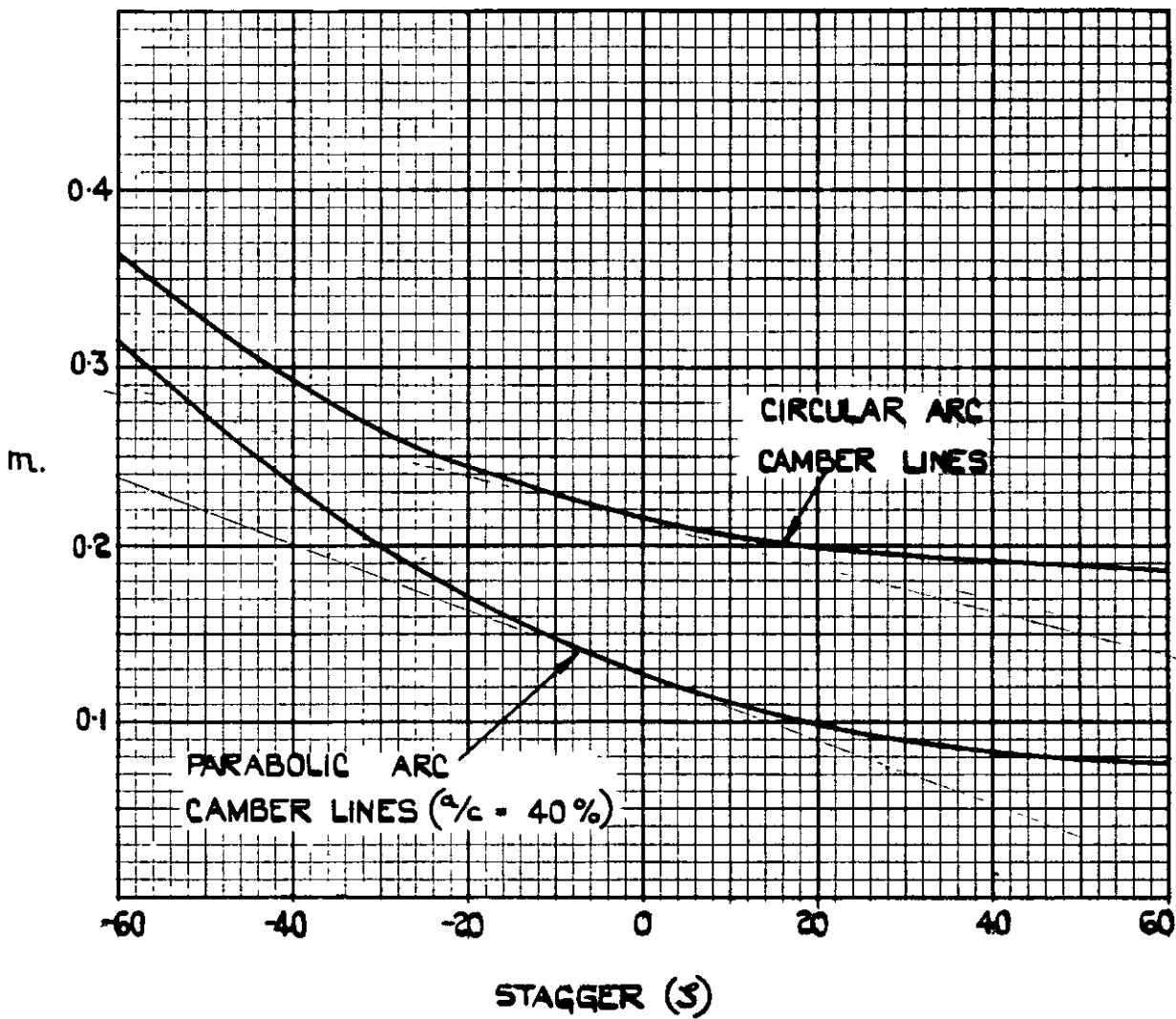
C1 C2 OR C4 BASE PROFILES HAVING 10% MAXIMUM THICKNESS ON CAMBER LINES AS INDICATED



12/24/52

FIG. 6.

DEVIATION RULE.

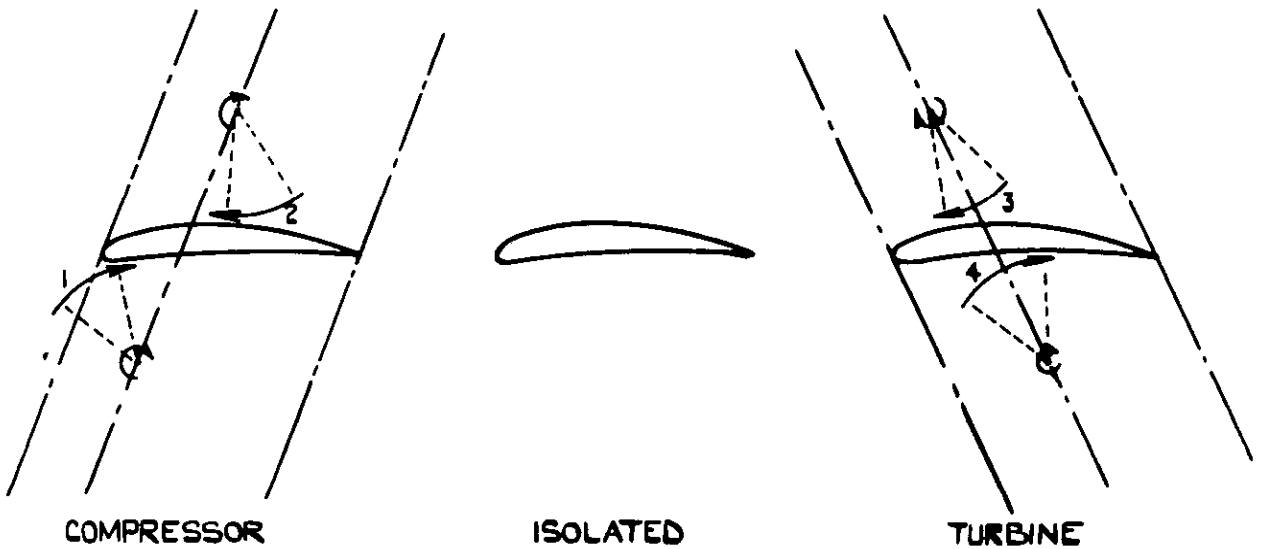


$$\delta^\circ = m \theta \sqrt{\frac{3}{c}} - \text{COMPRESSOR CASCADES}$$

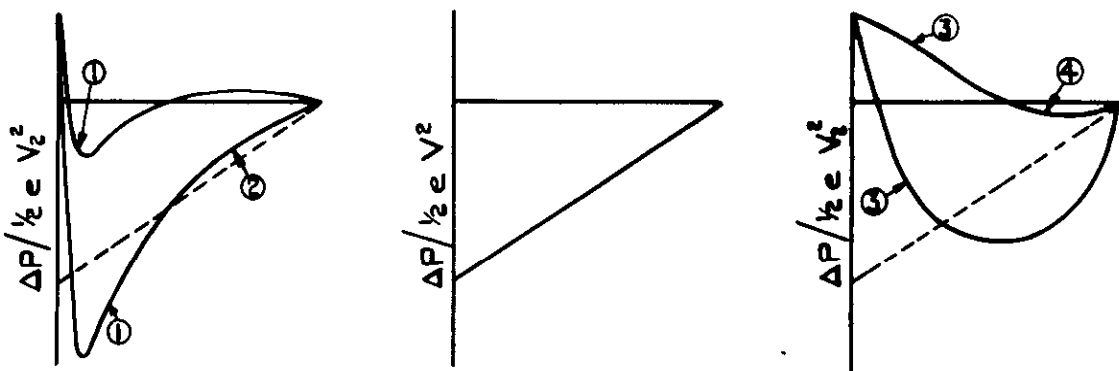
$$\delta^\circ = m \theta \frac{3}{c} - \text{TURBINE CASCADES.}$$

NOTE. δ° IS THE DEVIATION AT OPTIMUM INCIDENCE

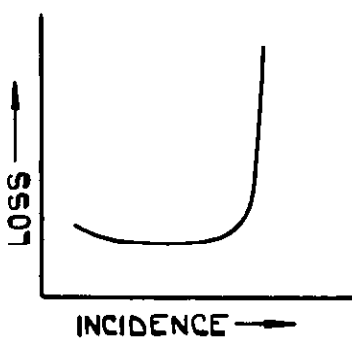
EFFECT OF STAGGER ON CASCADE PERFORMANCE.



(a) SCHEMATIC REPRESENTATION SHOWING MAJOR INTERFERENCE EFFECTS OF NEIGHBOURING AEROFOILS.

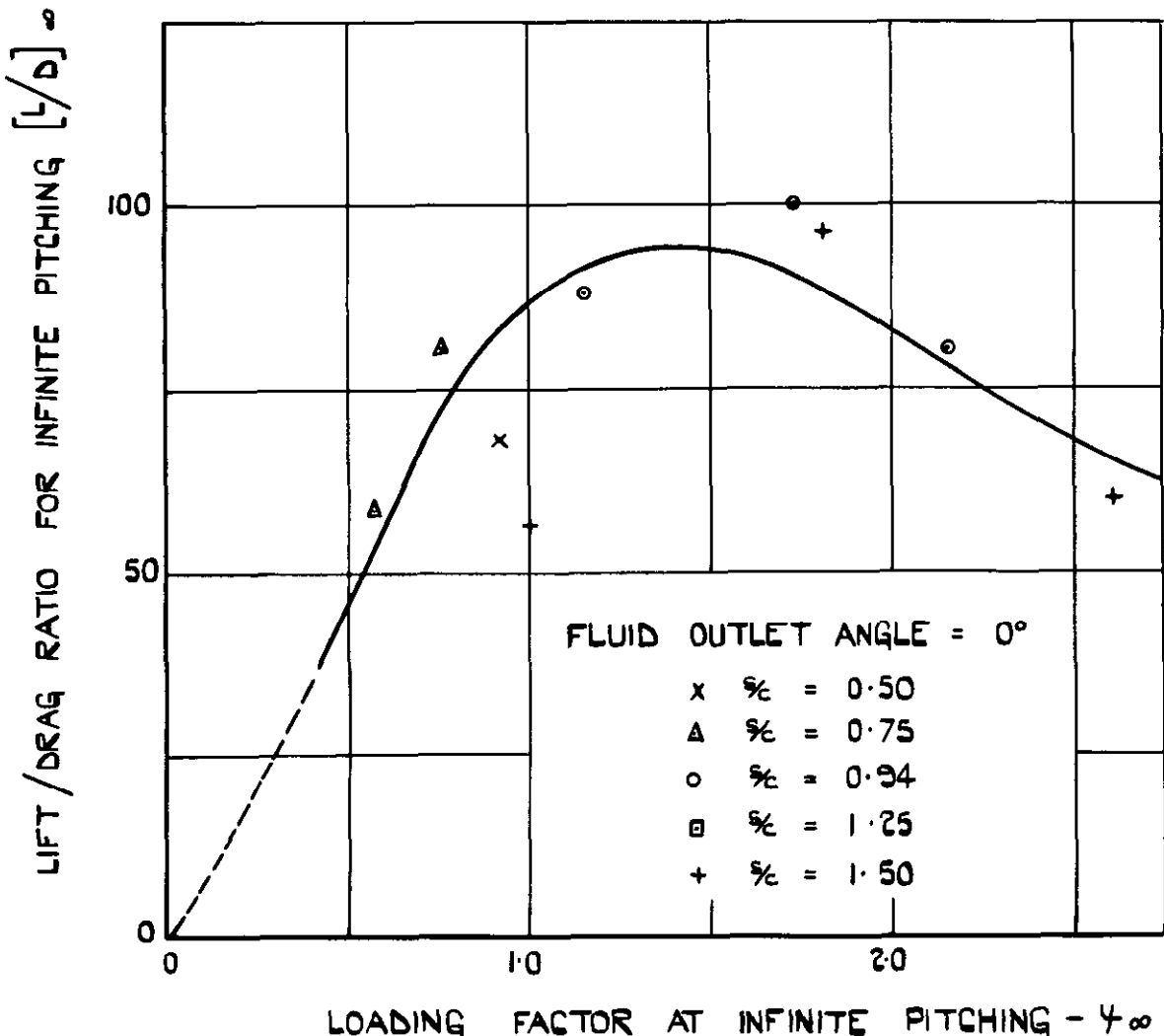
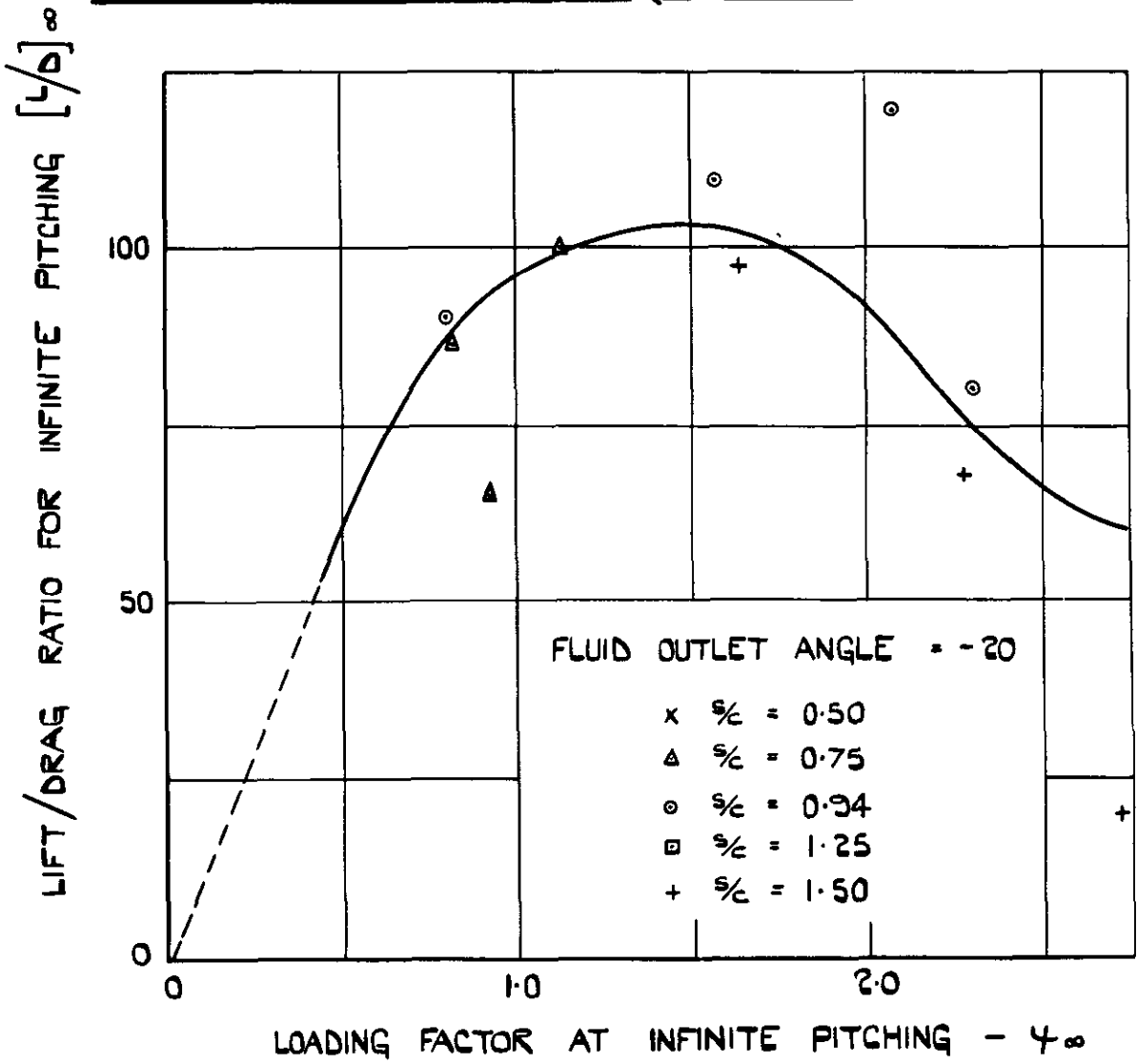


(b) PRESSURE DISTRIBUTIONS. ON UPPER SURFACE RESULTANT OF MAINSTREAM AND INDUCED VELOCITIES TENDS TO PRODUCE A CONCAVE PRESSURE DISTRIBUTION IN CASE OF COMPRESSOR CASCADE AND CONVEX DISTRIBUTION IN THE CASE OF A TURBINE CASCADE.

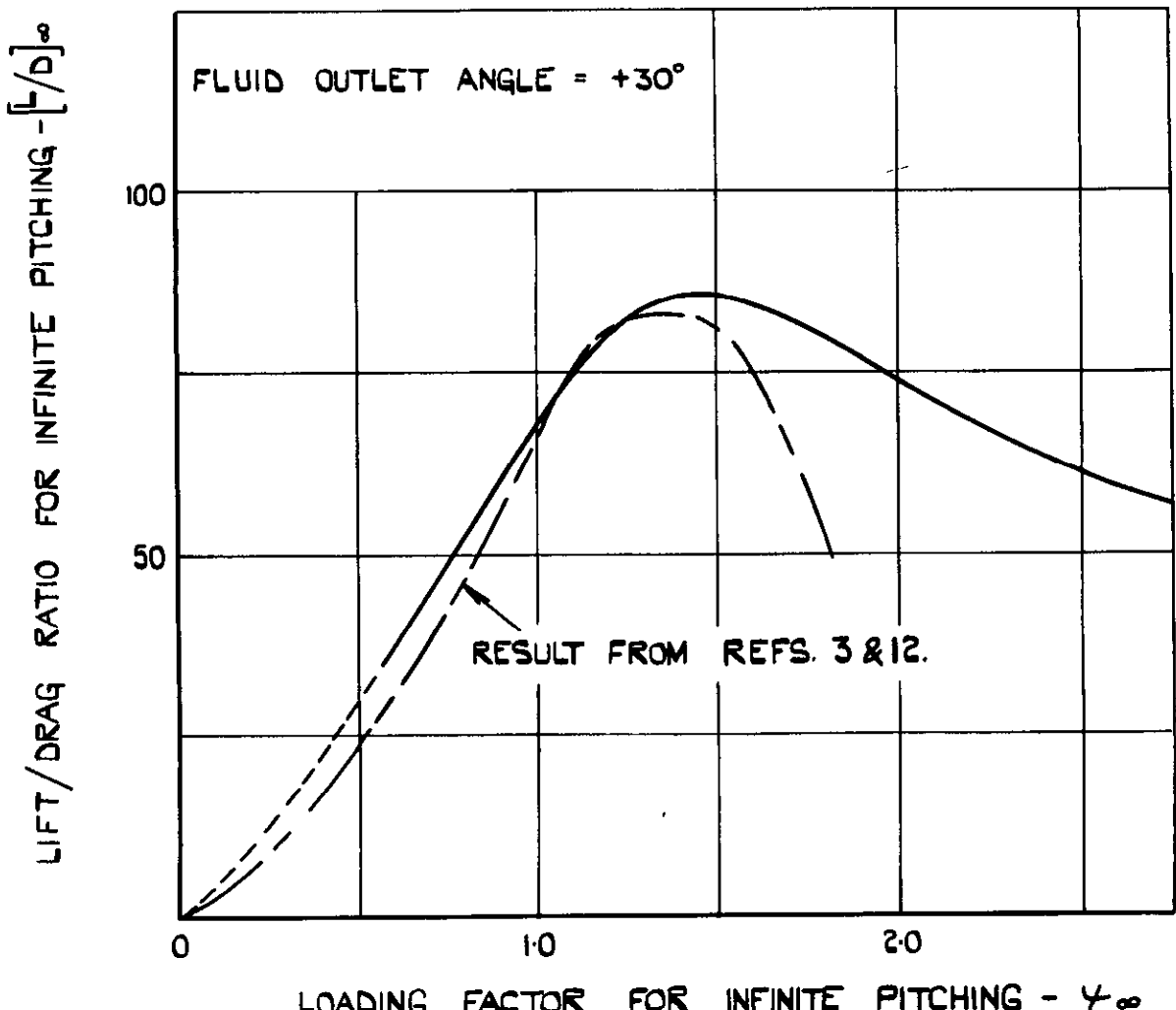
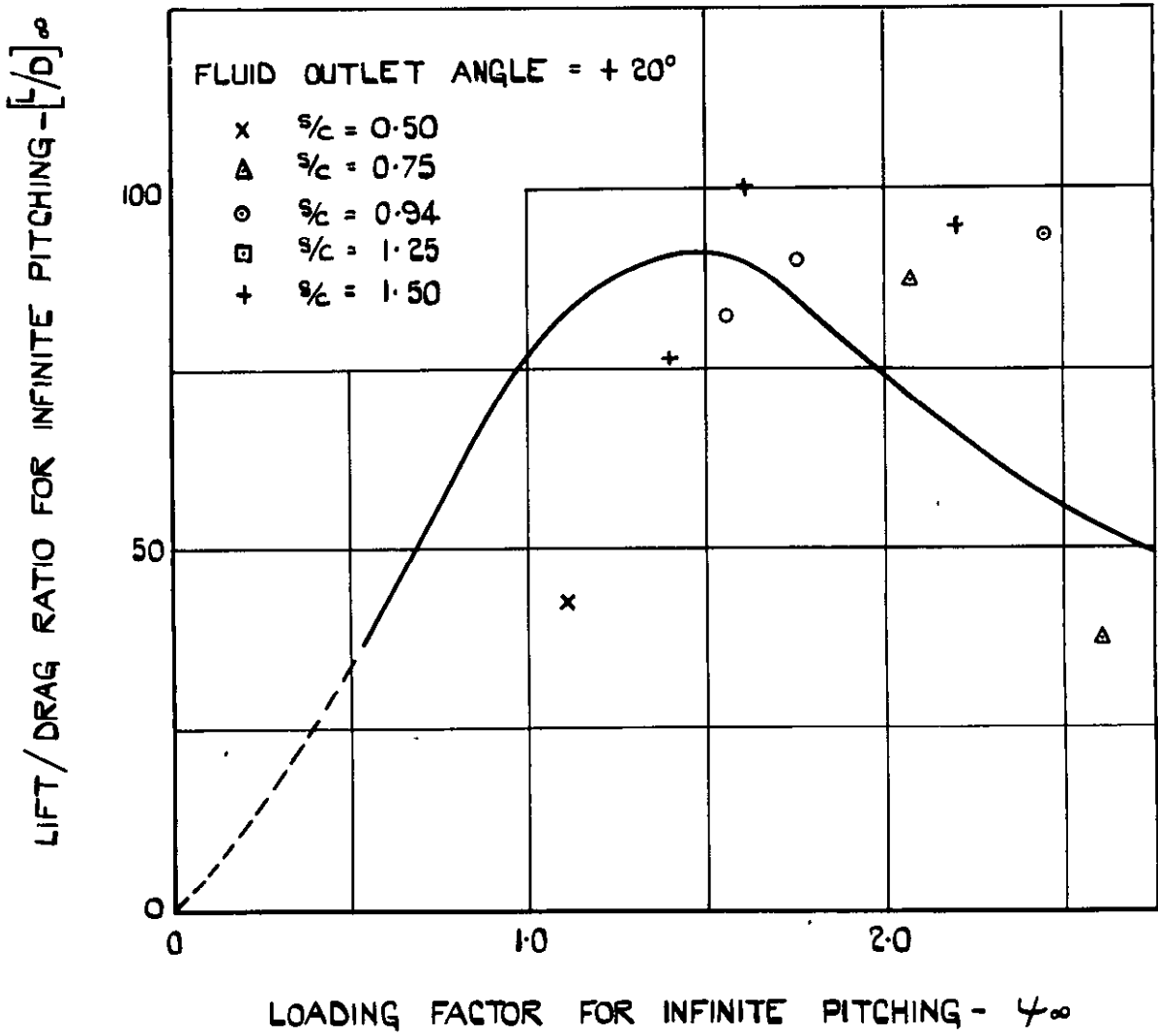


LOSS v INCIDENCE CURVES. PRESSURE DISTRIBUTIONS OF FIG. 6(b) WOULD INDICATE SUDDEN STALL FOR COMPRESSOR CASCADES AND SLOW STALL FOR TURBINES. ALSO LARGE REGION OF LAMINAR FLOW AND CONSEQUENTLY HIGH LIFT/DRAG RATIOS IN THIS CASE

LIFT DRAG RATIOS ($\alpha_2 = -20^\circ$ & $\alpha_2 = 0^\circ$)

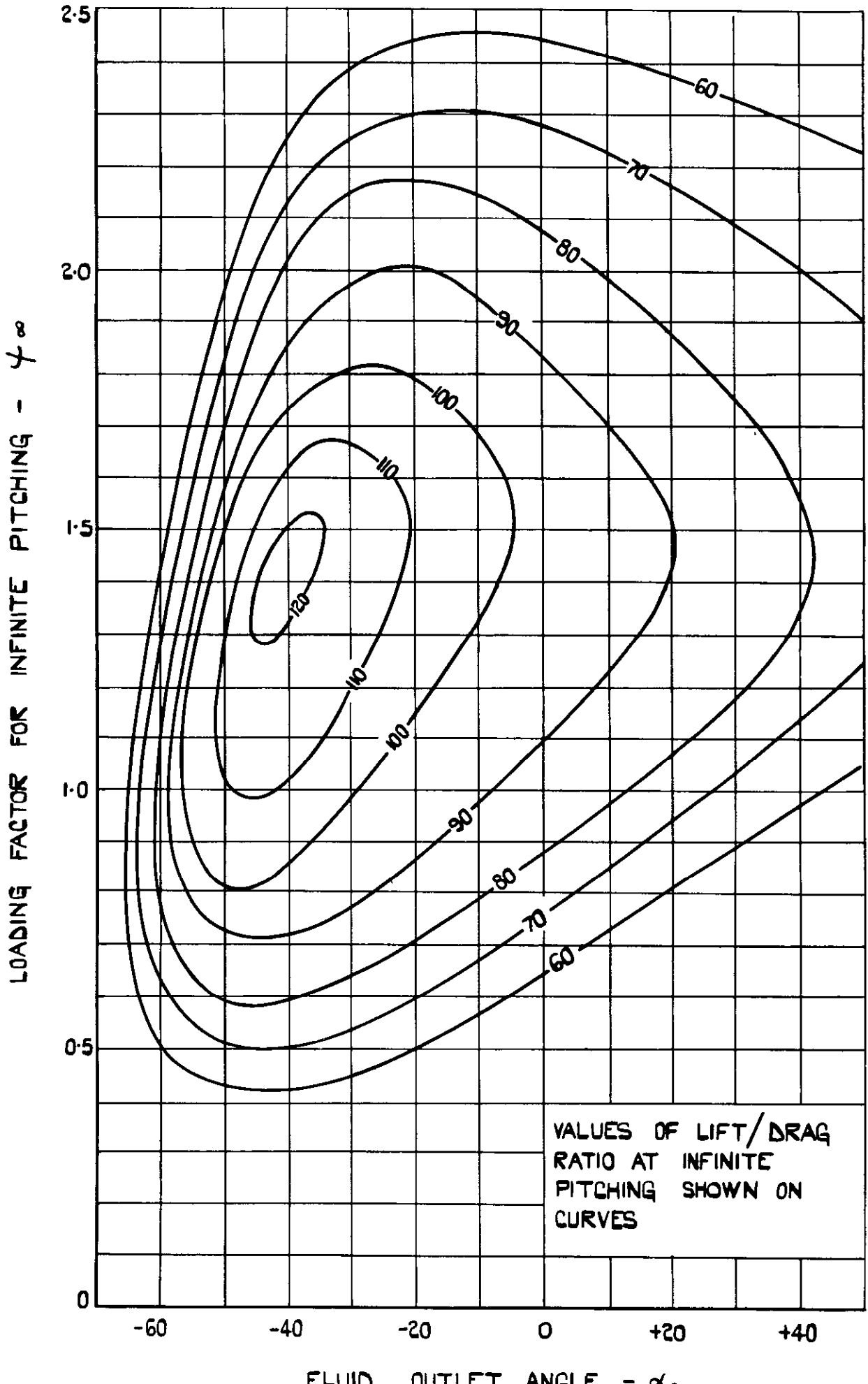


LIFT DRAG RATIOS ($\alpha_2 = +20^\circ$ & $\alpha_2 = +30^\circ$)

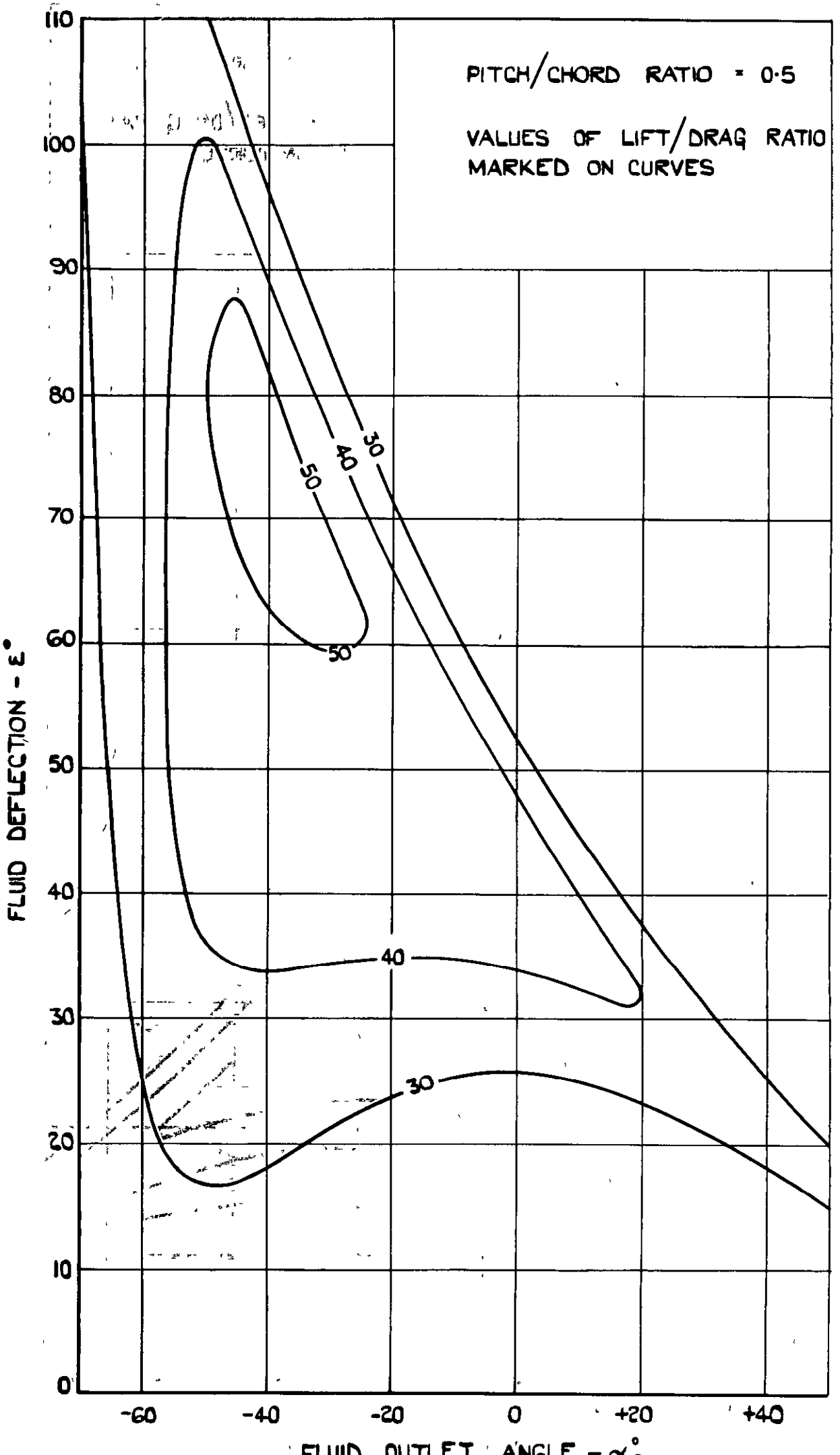


GENERAL PERFORMANCE CURVES.

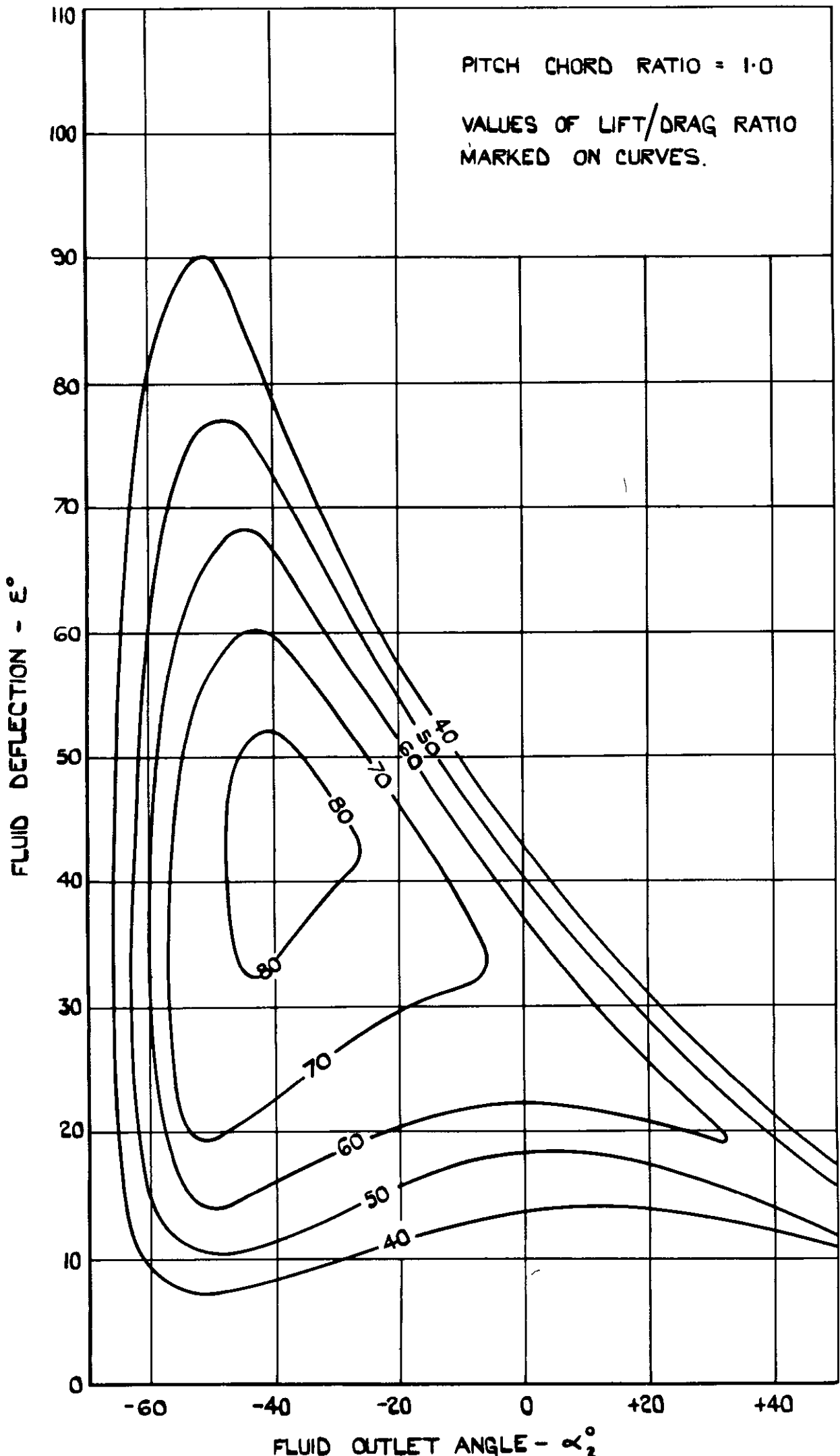
C1 C2 OR C4 BASE PROFILES ON CIRCULAR ARC CAMBER LINES. MAXIMUM THICKNESS 10% CHORD.



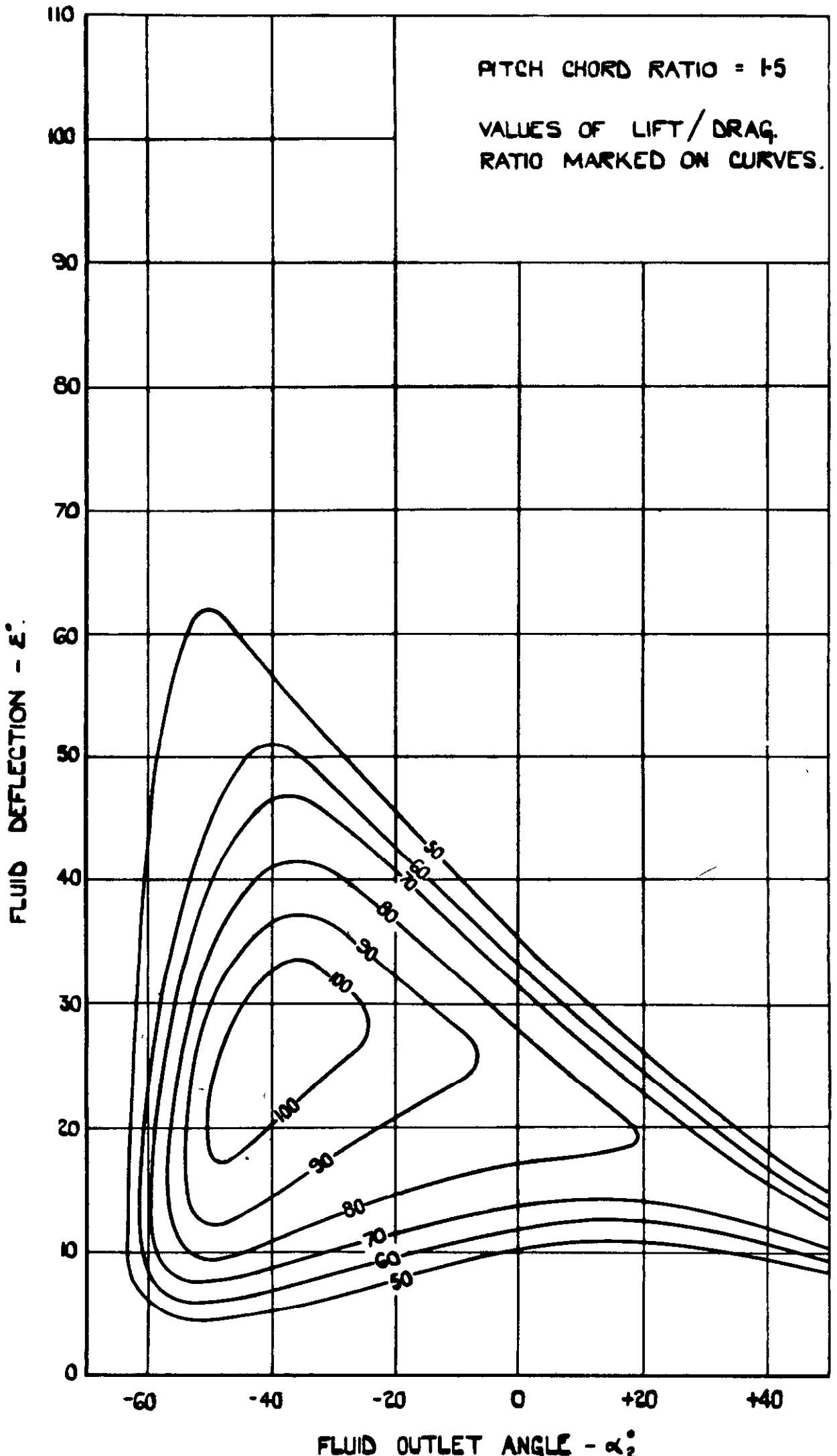
PERFORMANCE CURVES ($s/c = 0.5$)



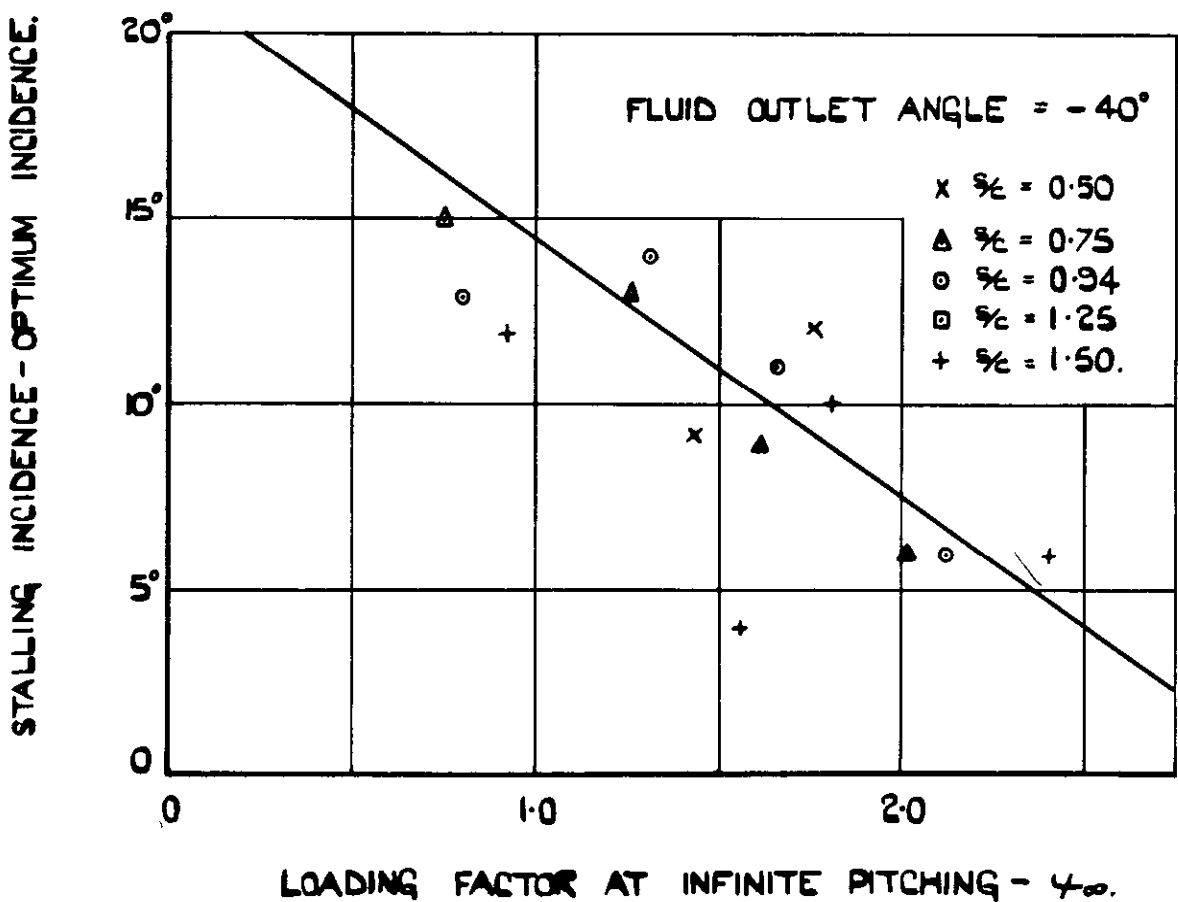
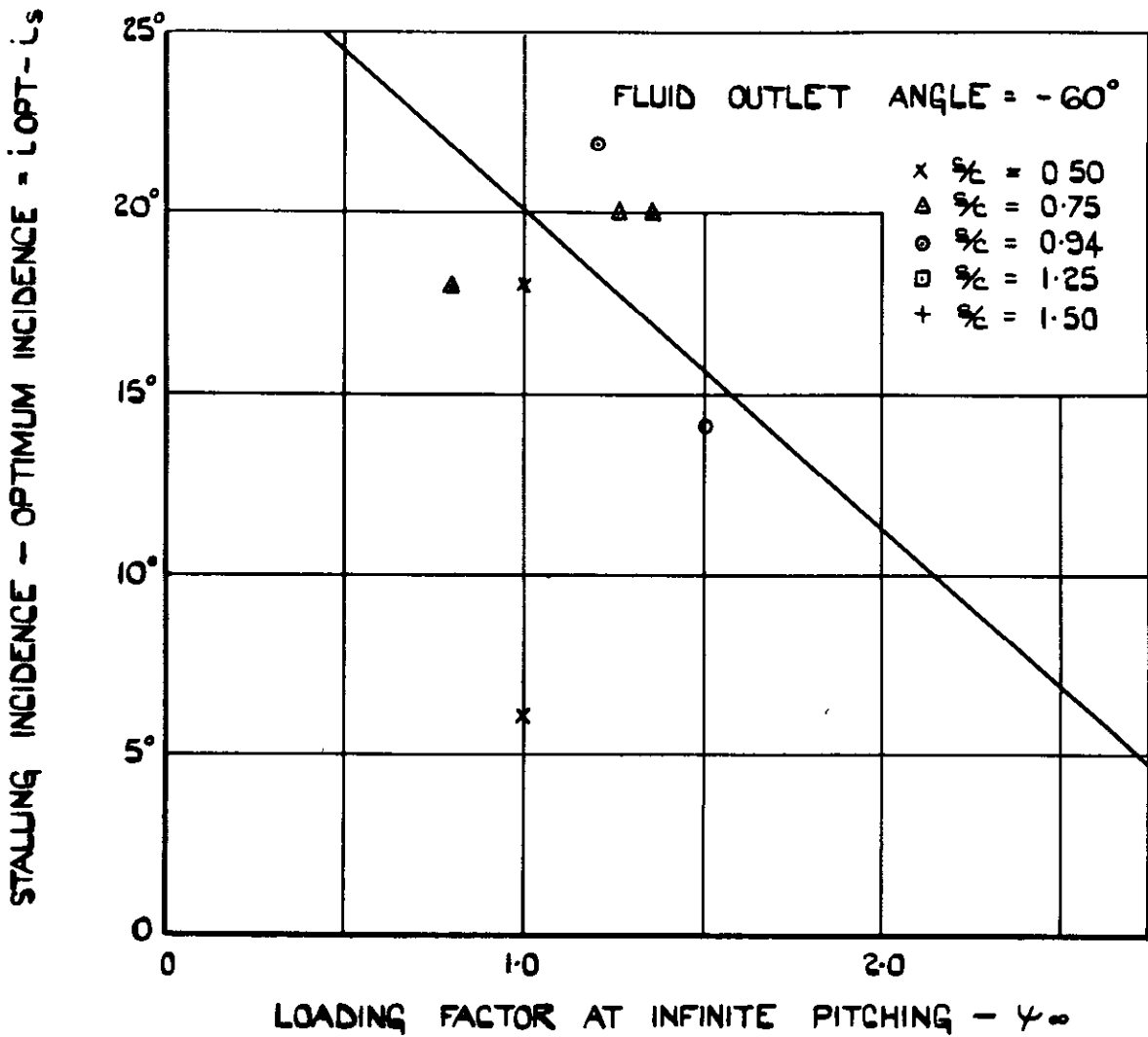
PERFORMANCE CURVES ($\frac{s}{c} = 1.0$)



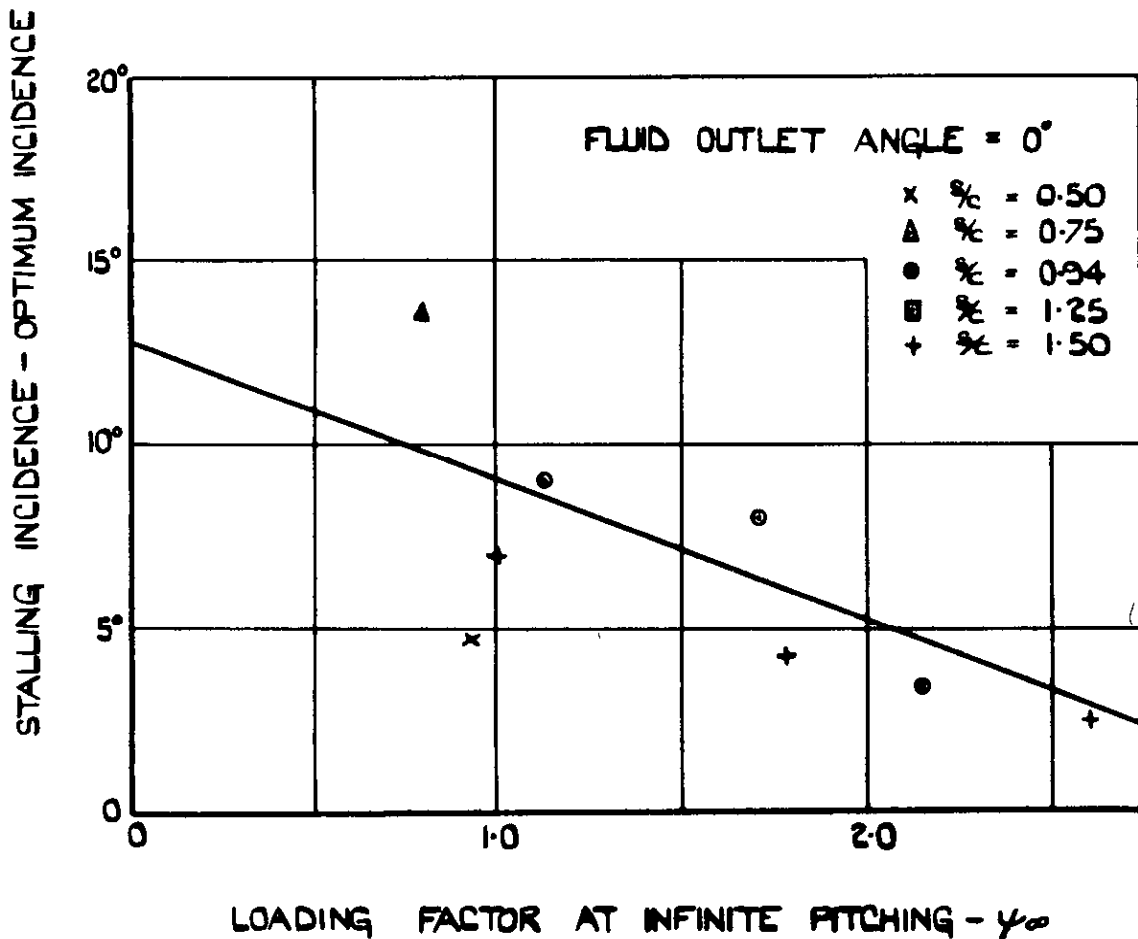
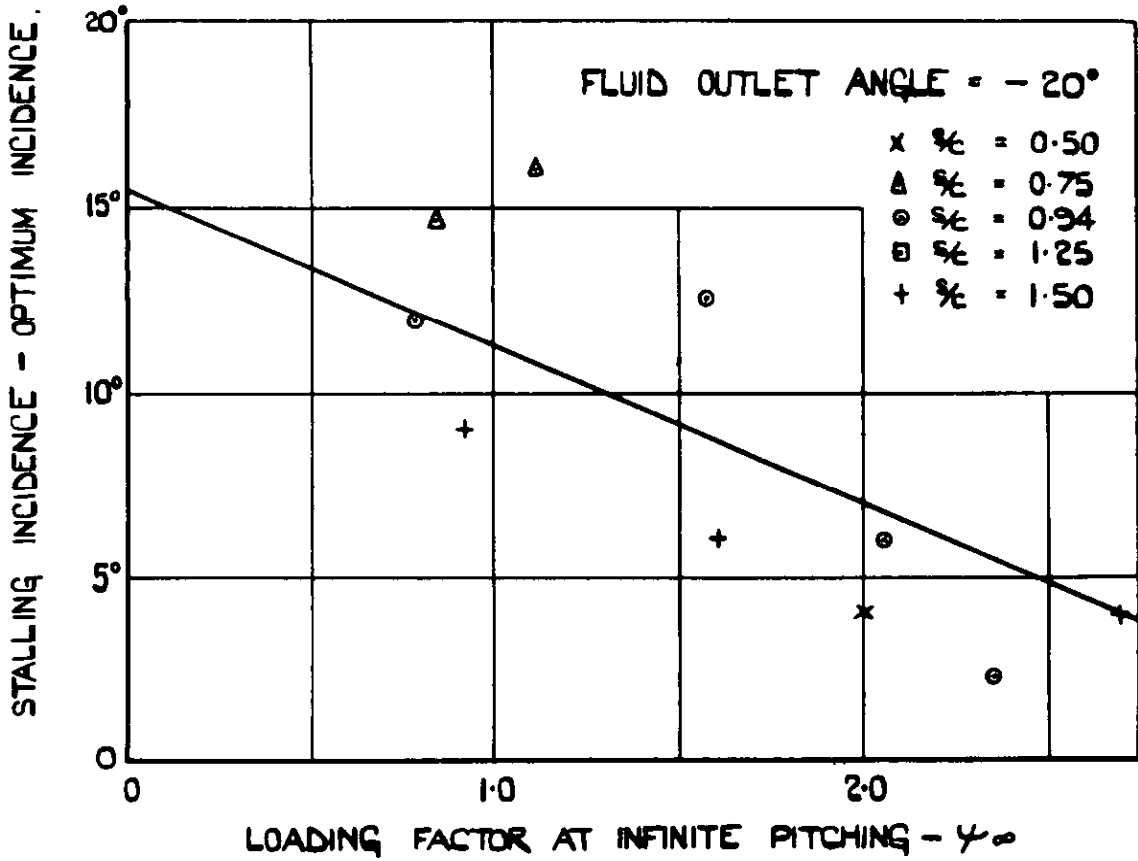
PERFORMANCE CURVES ($\frac{b}{c} = 1.5$)



INCIDENCE INCREMENT ($\alpha_2 = -60^\circ$ & $\alpha_2 = -40^\circ$)

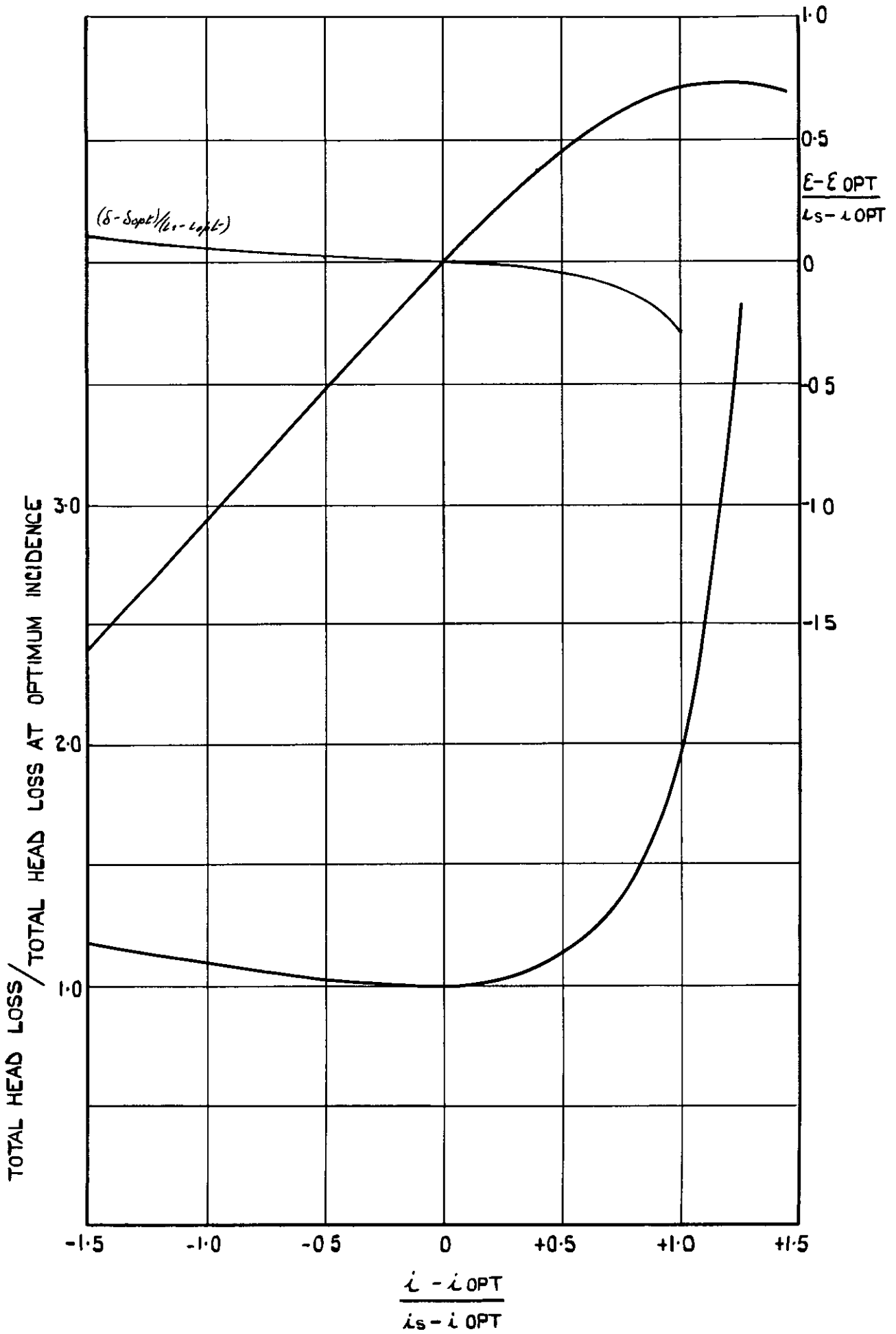


INCIDENCE INCREMENT ($\alpha_2 = -20^\circ$ & $\alpha_2 = 0^\circ$)

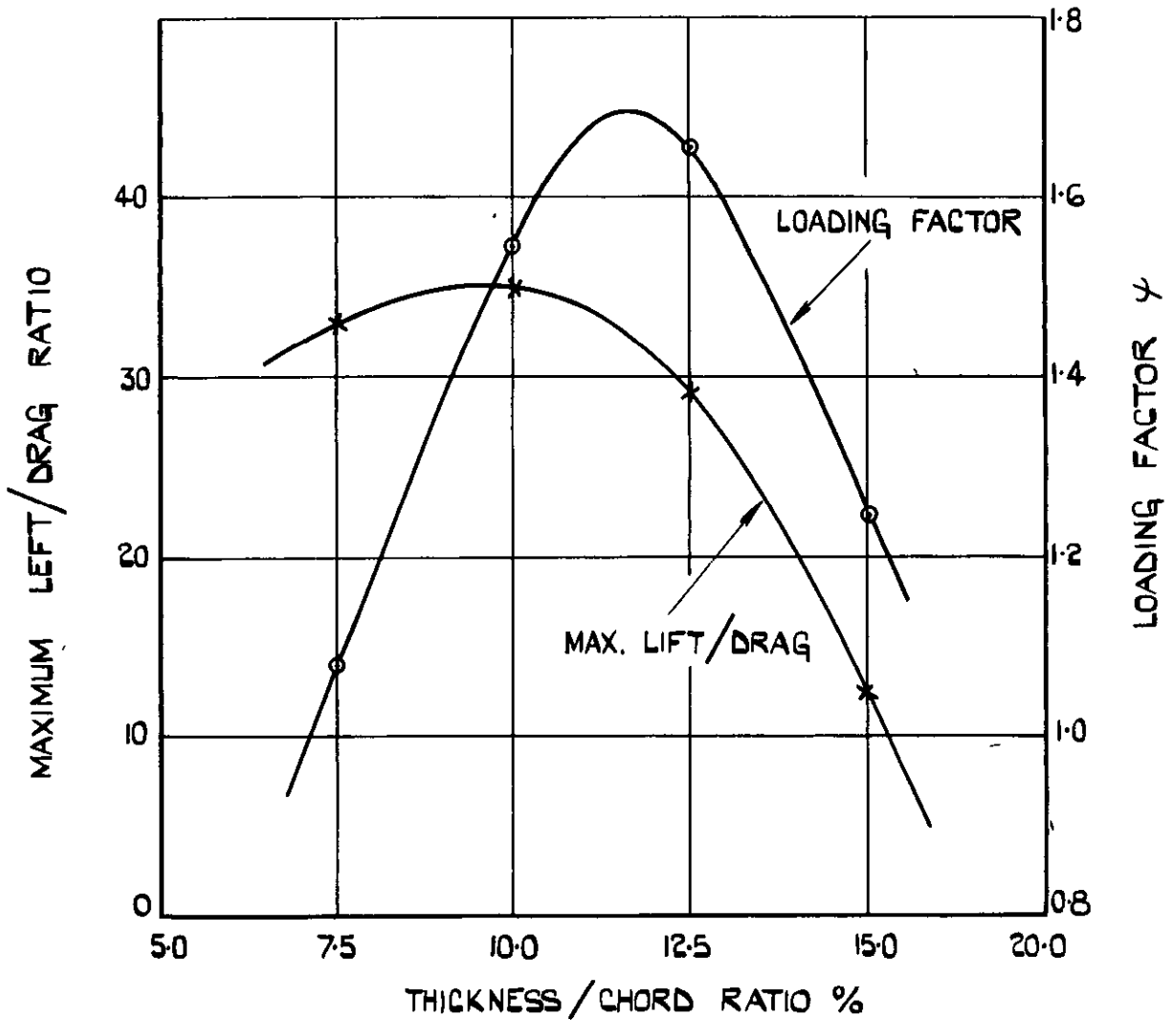


FLUID OUTLET ANGLE - α_2

LOSS & DEFLECTION v INCIDENCE.



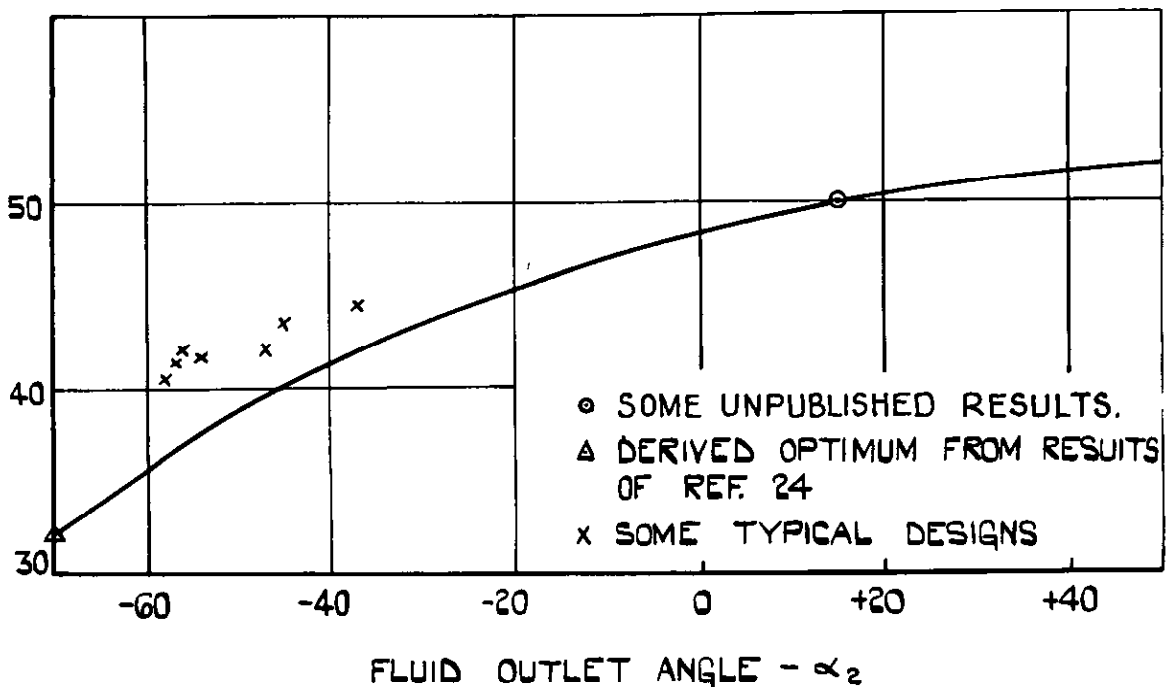
(a) EFFECT OF AERFOIL THICKNESS ON CASCADE PERFORMANCE.



(b) OPTIMUM POSITION OF MAXIMUM CAMBER

POSITION OF MAX. CAMBER FROM LE. (% C)

NOTE THIS IS A TENTATIVE CURVE AND SHOULD ONLY BE TREATED AS ILLUSTRATING GENERAL TENDANCIES



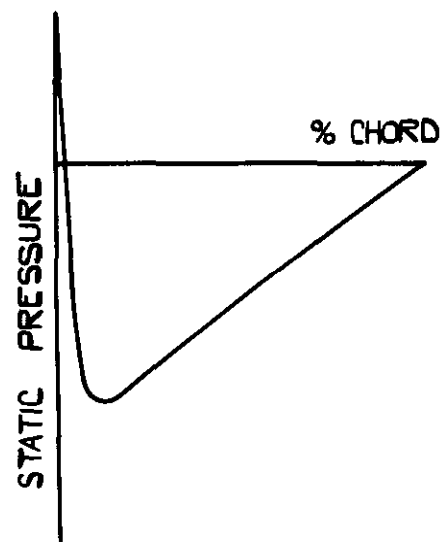
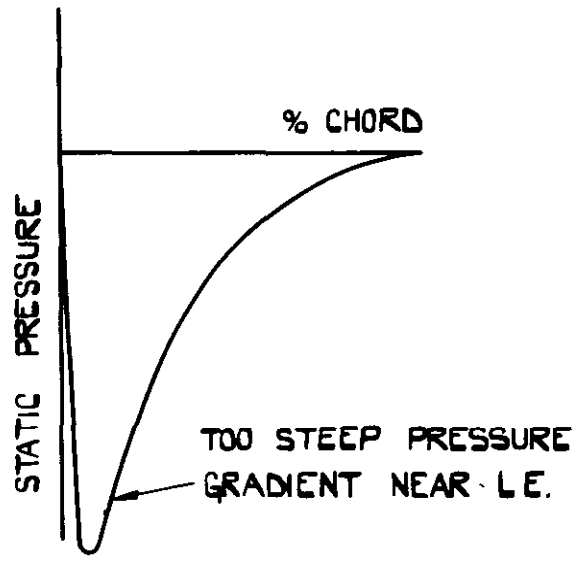
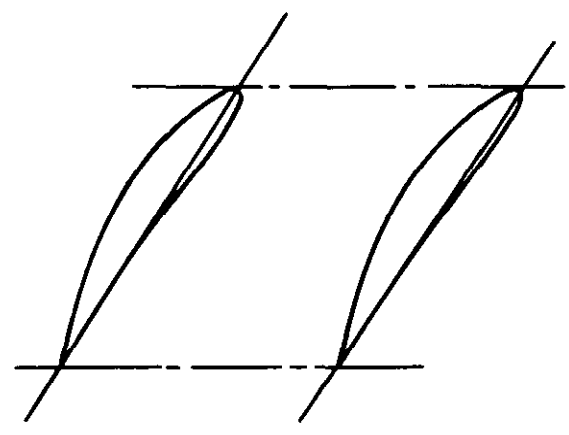
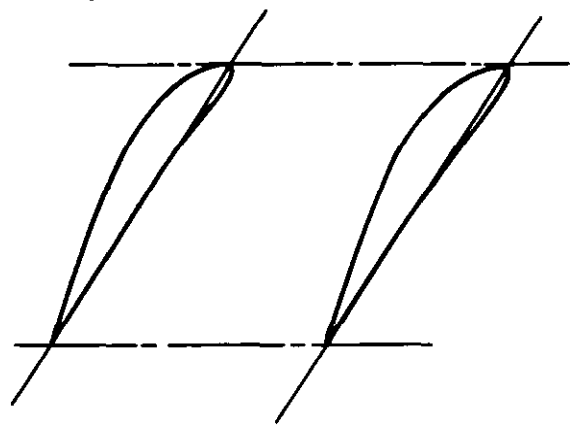
○ SOME UNPUBLISHED RESULTS.
 △ DERIVED OPTIMUM FROM RESULTS OF REF. 24
 x SOME TYPICAL DESIGNS

COMBINATIONS OF FLUID OUTLET ANGLE
AND POSITION OF MAXIMUM CAMBER.

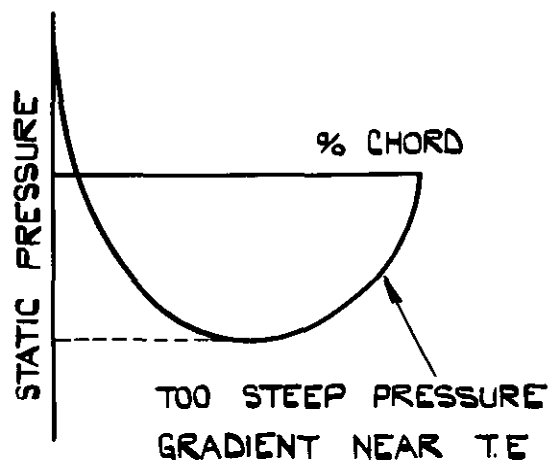
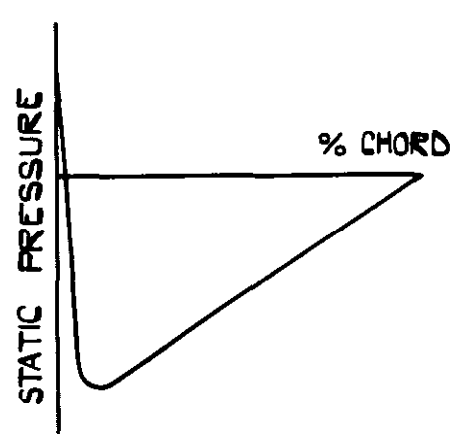
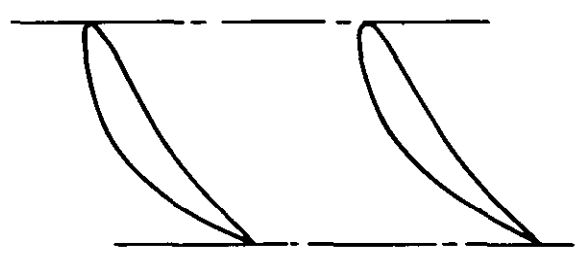
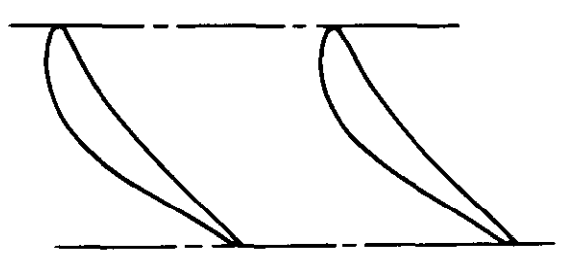
POSITION OF MAXIMUM
CAMBER WELL FORWARD.

POSITION OF MAXIMUM
CAMBER TOWARDS REAR.

(a) HIGH FLUID OUTLET ANGLE

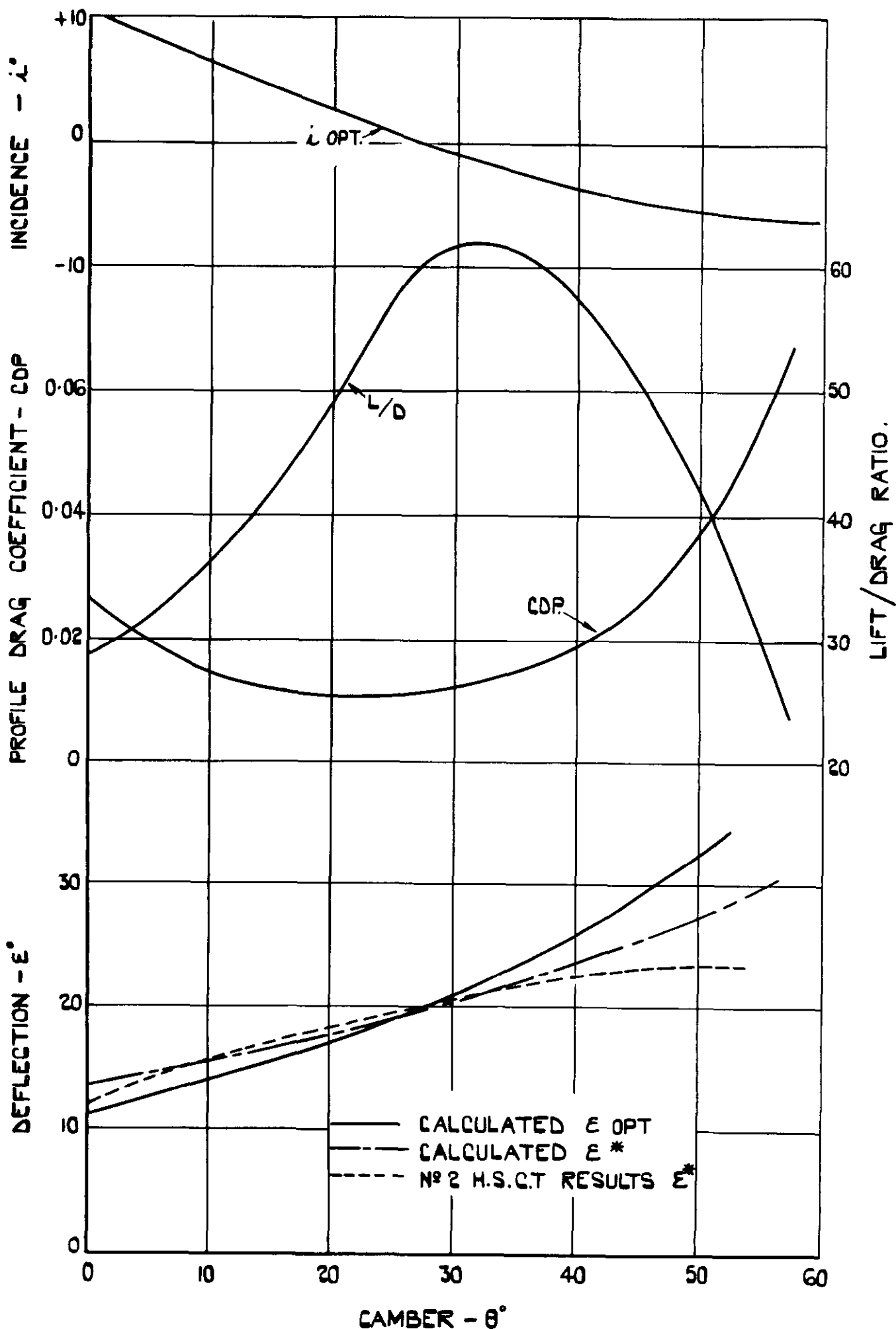


(b) LOW FLUID OUTLET ANGLE.



CASCADE PERFORMANCE.

{ FLUID OUTLET ANGLE = 20°
 { PITCH CHORD RATIO = 1.0



COMPARISON OF TEST AND CALCULATED CHARACTERISTICS.

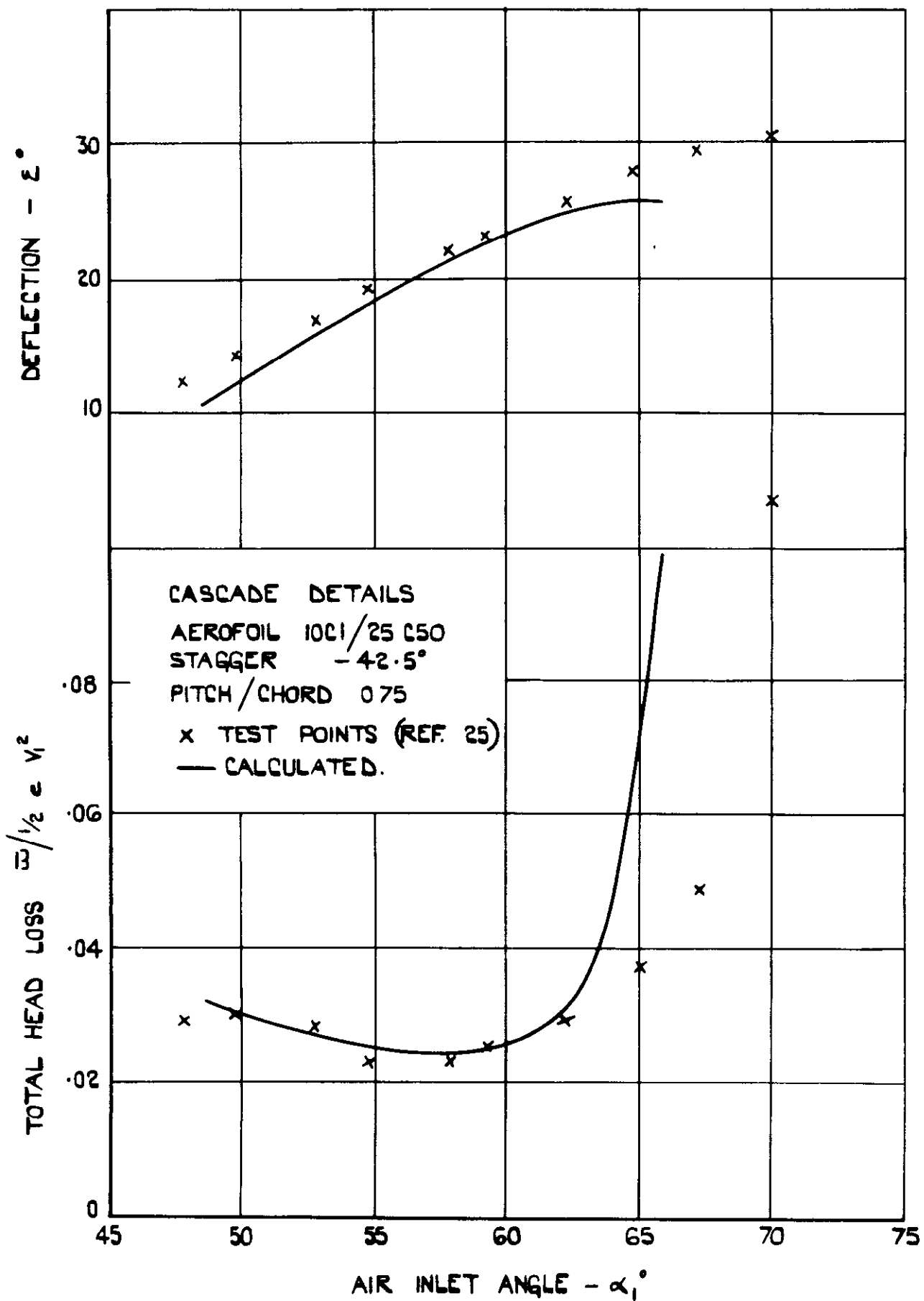
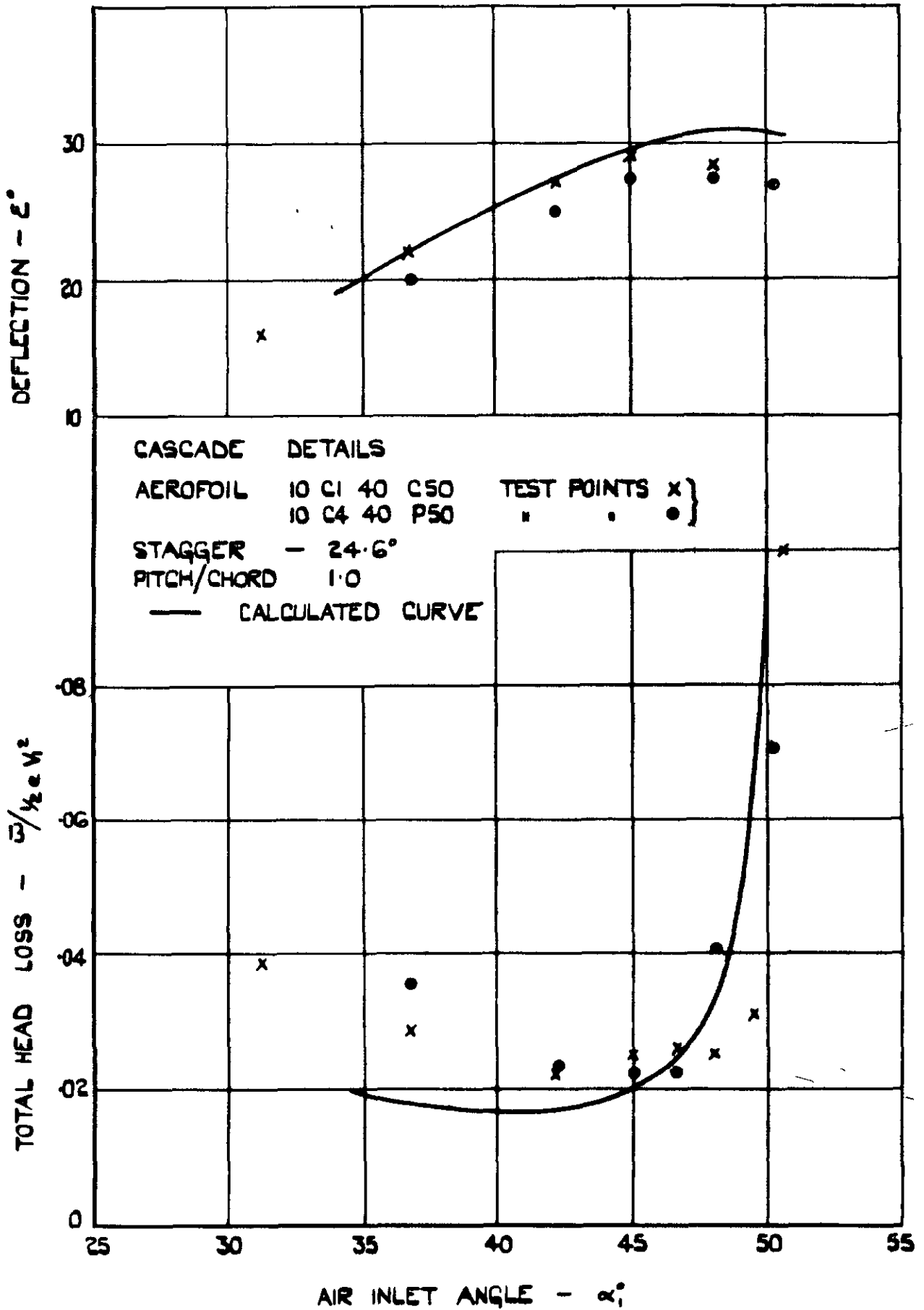
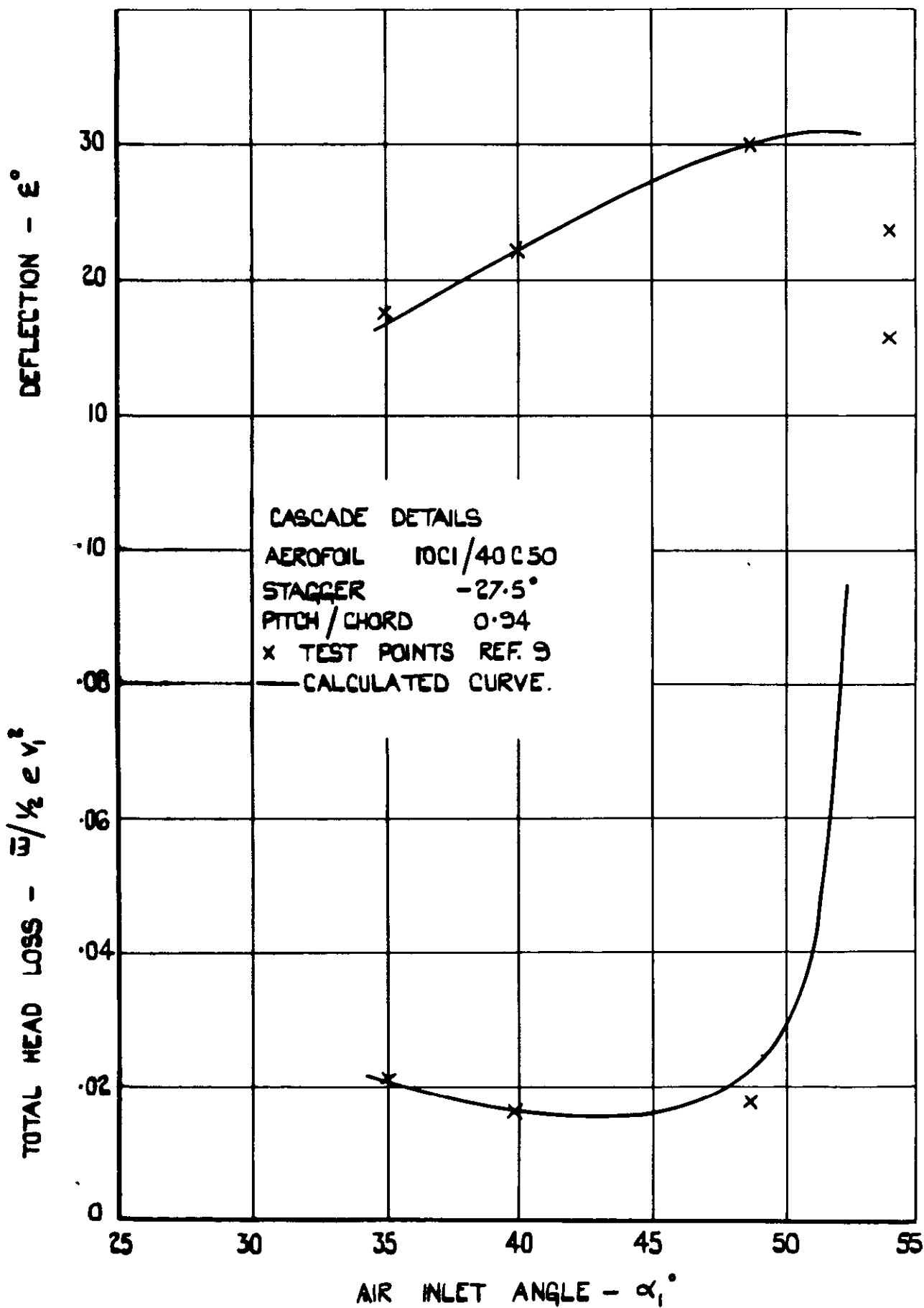


FIG. 25.

COMPARISON OF TEST AND CALCULATED
CHARACTERISTICS.



COMPARISON OF TEST AND CALCULATED CHARACTERISTICS.





C P No 29
(12,883)
A.R.C Technical Report

PRINTED AND PUBLISHED BY HIS MAJESTY'S STATIONERY OFFICE

To be purchased from

York House, Kingsway, LONDON, W C 2 429 Oxford Street, LONDON, W 1

P O BOX 569, LONDON, S E 1

13a Castle Street, EDINBURGH, 2 1 St Andrew's Crescent, CARDIFF

39 King Street, MANCHESTER, 2 Tower Lane, BRISTOL, 1

2 Edmund Street, BIRMINGHAM, 3 80 Chichester Street, BELFAST

or from any Bookseller

1950

Price 3s 6d net

PRINTED IN GREAT BRITAIN

S.O. Code No. 23-9006-29